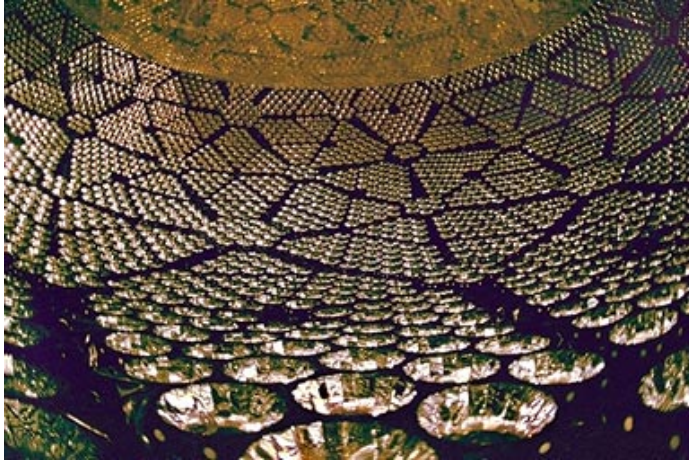


First Solar Neutrino Results from the Sudbury Neutrino Observatory

Andrew Hime
for the SNO Collaboration
Physics Division, Los Alamos National Laboratory

With Special Thanks and Appreciation to LANL for more than a Decade of
Support, Patience, and Encouragement!

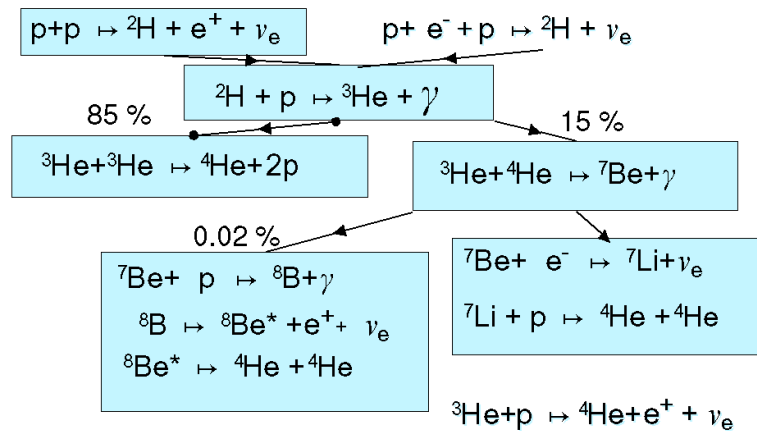


Sudbury Neutrino Observatory

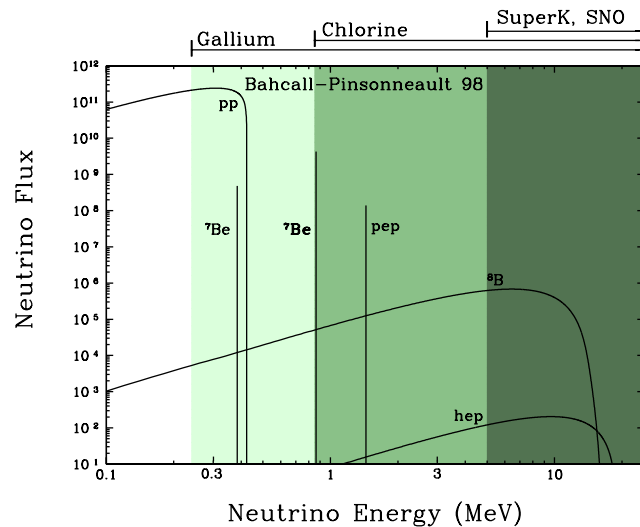
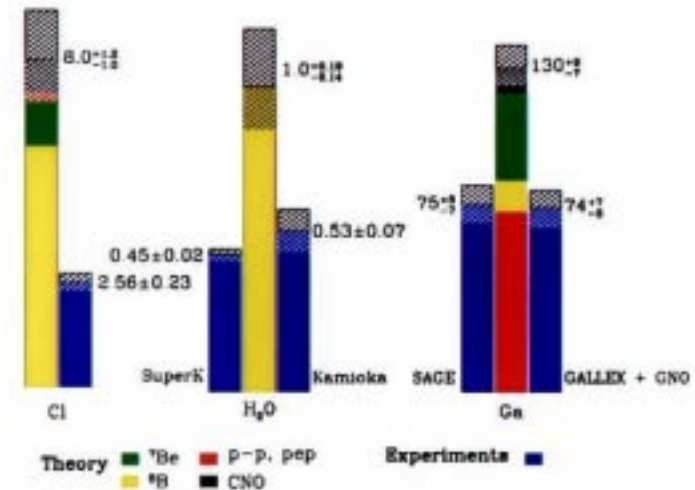
- Introduction and Overview
- Calibration and Detector Response
- Instrumental & Radioactive Background
- Data Analysis
- Interpretation of Results
- Future Plans & Outlook



The Solar Neutrino Problem



Total Rates: Standard Model vs. Experiment
Bahcall-Pinsonneault 00



Solar Models are Incomplete
or Incorrect

Or

Neutrinos Experience Flavor
Changing Oscillations

So it Appears that the Sun Shines Underground ...

But Apparently Less Brightly Than on the Surface.

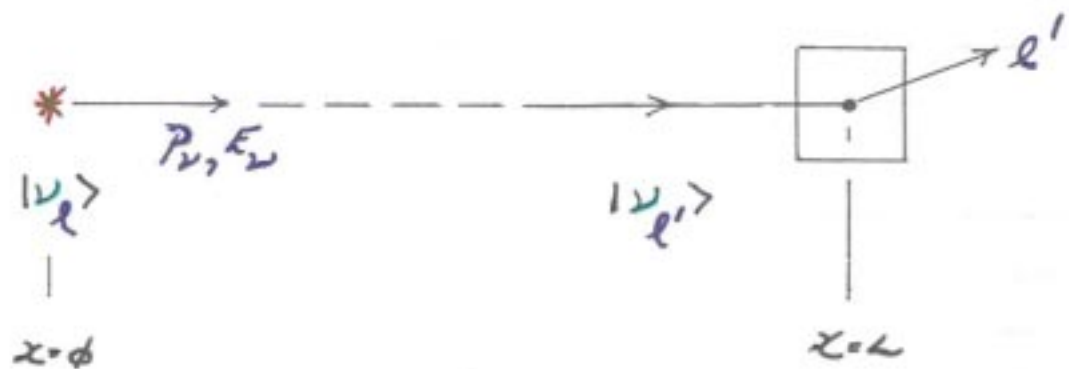
Allow ν -Mass Beyond the Standard Model.

$$\therefore |\nu_\ell\rangle = \sum_i U_{\ell i} |\nu_i\rangle$$

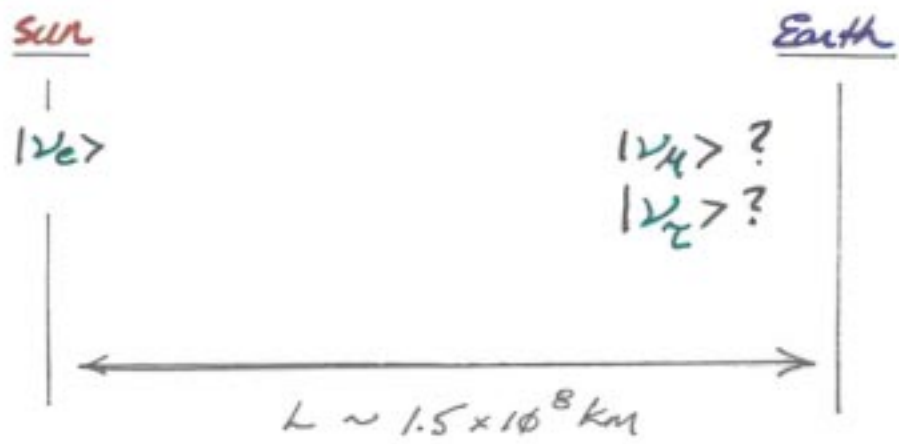
\swarrow "weak" interaction eigenstates
 $\ell = e, \mu, \tau$

\downarrow unitary mixing matrix

\searrow "mass" eigenstates
 $i = 1, 2, 3$



Example :



Only ν_e Produced in Sun

Existing Detectors Sensitive to Only ν_e !

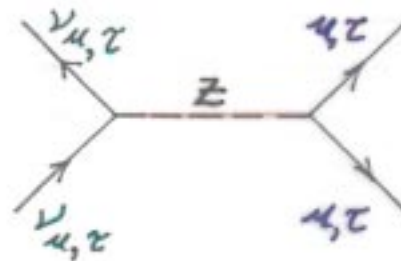
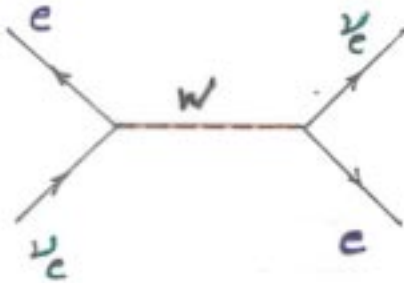
2 - Component Mixing

$$\begin{bmatrix} \nu_e \\ \nu_\mu \end{bmatrix} = \begin{bmatrix} \cos\theta & \sin\theta \\ -\sin\theta & \cos\theta \end{bmatrix} \cdot \begin{bmatrix} \nu_1 \\ \nu_2 \end{bmatrix}$$

$$P(\nu_e \leftrightarrow \nu_\mu; L) = \sin^2 2\theta \sin^2\left(\pi \frac{L}{L_0}\right) ,$$

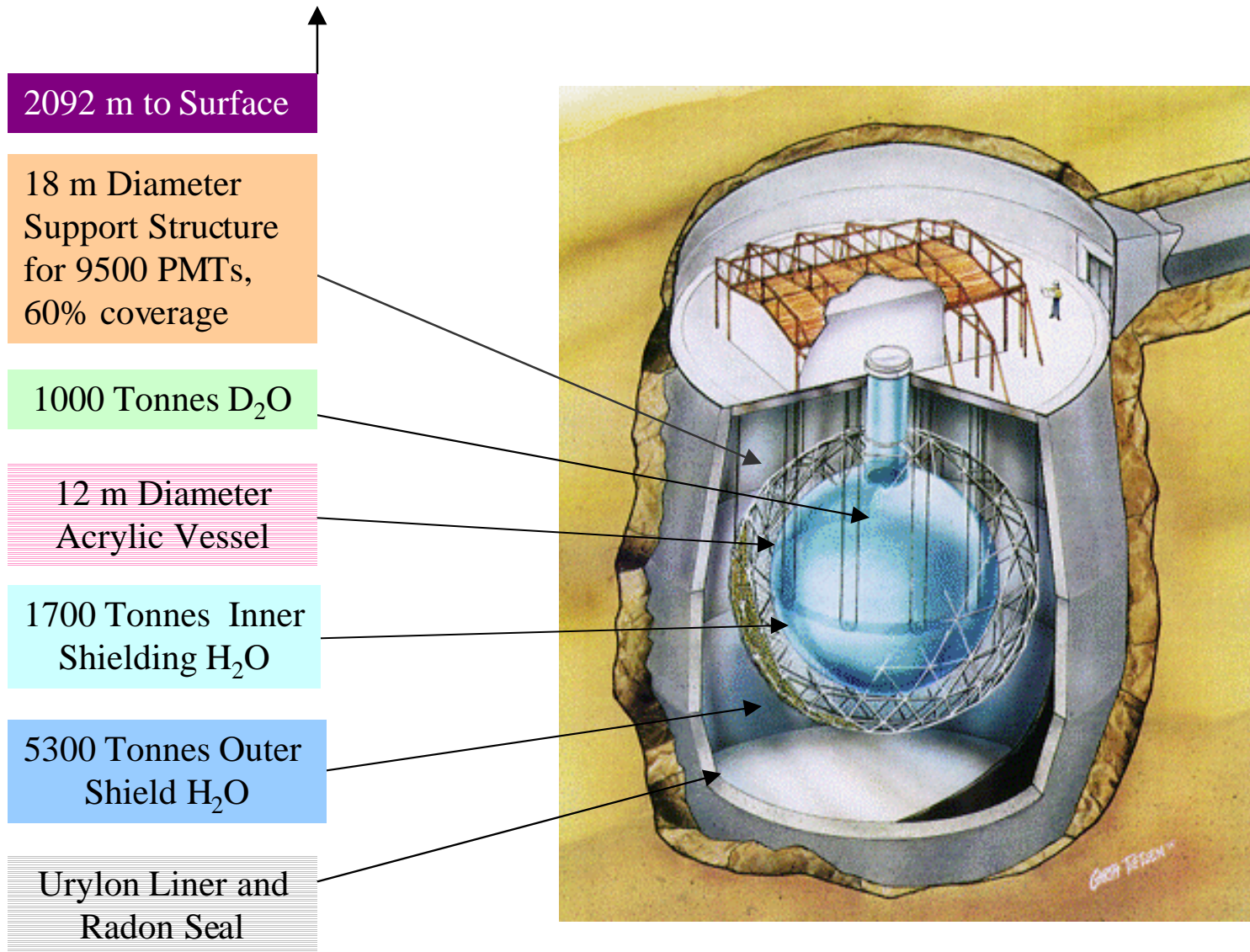
$$L_0 = 4\pi \frac{P_L}{|m_2^2 - m_1^2|} .$$

Matter Enhanced ν -Oscillations (MSW)



$$\sin^2 2\theta_p = \frac{\sin^2 2\theta}{\left[\cos 2\theta - \frac{L_0}{L_p} \right] + \sin^2 2\theta}$$

Sudbury Neutrino Observatory





SNO Collaboration

J. Boger, R. L Hahn, J.K. Rowley, M. Yeh
Brookhaven National Laboratory

I. Blevis, F. Dalnoki-Veress, W. Davidson, J. Farine, D.R. Grant,
C. K. Hargrove, I. Levine, K. McFarlane, C. Mifflin, T. Noble,
V.M. Novikov, M. O'Neill, M. Shatkay, D. Sinclair, N. Starinsky
Carleton University

J. Bigu, J.H.M. Cowan, E. D. Hallman, R.U. Haq, J. Hewett, J.G.
Hykawy, G. Jonkmans, A. Roberge, E. Saettler, M.H.
Schwendener, H. Seifert, R. Tafirout, C. J. Virtue.
Laurentian University

Y. D. Chan, X. Chen, M. C. P. Isaac, K. T. Lesko, A. D. Marino,
E. B. Norman, C. E. Okada, A. W. P. Poon, A. R. Smith, A.
Schülke, R. G. Stokstad.

Lawrence Berkeley National Laboratory

T. J. Bowles, S. J. Brice, M. Dragowsky, M.M. Fowler, A.
Goldschmidt, A. Hamer, A. Hime, K. Kirch, G.G. Miller, J.B.
Wilhelmy, J.M. Wouters.

Los Alamos National Laboratory

E. Bonvin, M.G. Boulay, M. Chen, F.A. Duncan, E.D. Earle, H.C.
Evans, G.T. Ewan, R.J. Ford, A.L. Hallin, P.J. Harvey, J.D.
Hepburn, C. Jillings, H.W. Lee, J.R. Leslie, H.B. Mak, A.B.
McDonald, W. McLatchie, B. Moffat, B.C. Robertson, P.
Skensved, B. Sur.
Queen's University

S. Gil, J. Heise, R. Helmer, R.J. Komar, T. Kutter, C.W. Nally, H.S.
Ng, Y. Tserkovnyak, C.E. Waltham.

University of British Columbia

T.C. Andersen, M.C. Chon, P. Jagam, J. Law, I.T. Lawson, R. W.
Ollerhead, J. J. Simpson, N. Tagg, J.X. Wang

University of Guelph

J.C. Barton, S.Biller, R. Black, R. Boardman, M. Bowler, J. Cameron,
B. Cleveland, X. Dai, G. Doucas, J. Dunmore, H. Fergani, A.P. Ferraris,
K.Frame, H. Heron, C. Howard, N.A. Jelley, A.B. Knox, M. Lay, W.
Locke, J. Lyon, S. Majerus, N. McCaulay, G. McGregor, M. Moorhead,
M. Omori, N.W. Tanner, R. Taplin, M. Thorman, P. Thornewell. P.T.
Trent, D.L.Wark, N. West, J. Wilson

University of Oxford

E. W. Beier, D. F. Cowen, E. D. Frank, W. Frati, W.J. Heintzelman,
P.T. Keener, J. R. Klein, C.C.M. Kyba, D. S. McDonald, M.S.Neubauer,
F.M. Newcomer, S. Oser, V. Rusu, R. Van Berg, R.G. Van de Water, P.
Wittich.

University of Pennsylvania

Q.R. Ahmad, M.C. Browne, T.V. Bullard, P.J. Doe, C.A. Duba, S.R.
Elliott, R. Fardon, J.V. Germani, A.A. Hamian, R. Hazama, K.M.
Heeger, M. Howe, R. Meijer Drees, J.L. Orrell, R.G.H. Robertson, K.
Schaffer, M.W.E. Smith, T.D. Steiger, J.F. Wilkerson.

University of Washington

R.G. Allen, G. Buhler, **H.H. Chen***
University of California, Irvine

* Deceased

Solar Neutrino Reactions

Charged Current Reaction (D₂O):

CC



(Only ν_e)

- ν_e flux and energy spectrum
- Some directional sensitivity ($1 - 1/3 \cos \theta_e$)

Neutral Current Reaction (D₂O):

NC



(All ν types)

- Total active neutrino flux

Elastic Scattering Reaction (D₂O, H₂O):

ES



(Mostly ν_e)

- Directional sensitivity (forward peaked)

SNO Provides a Model-Independent Test of Neutrino Oscillations via ES/CC, NC/CC, and CC-Shape

The Three Phases of SNO

I. Pure-D20

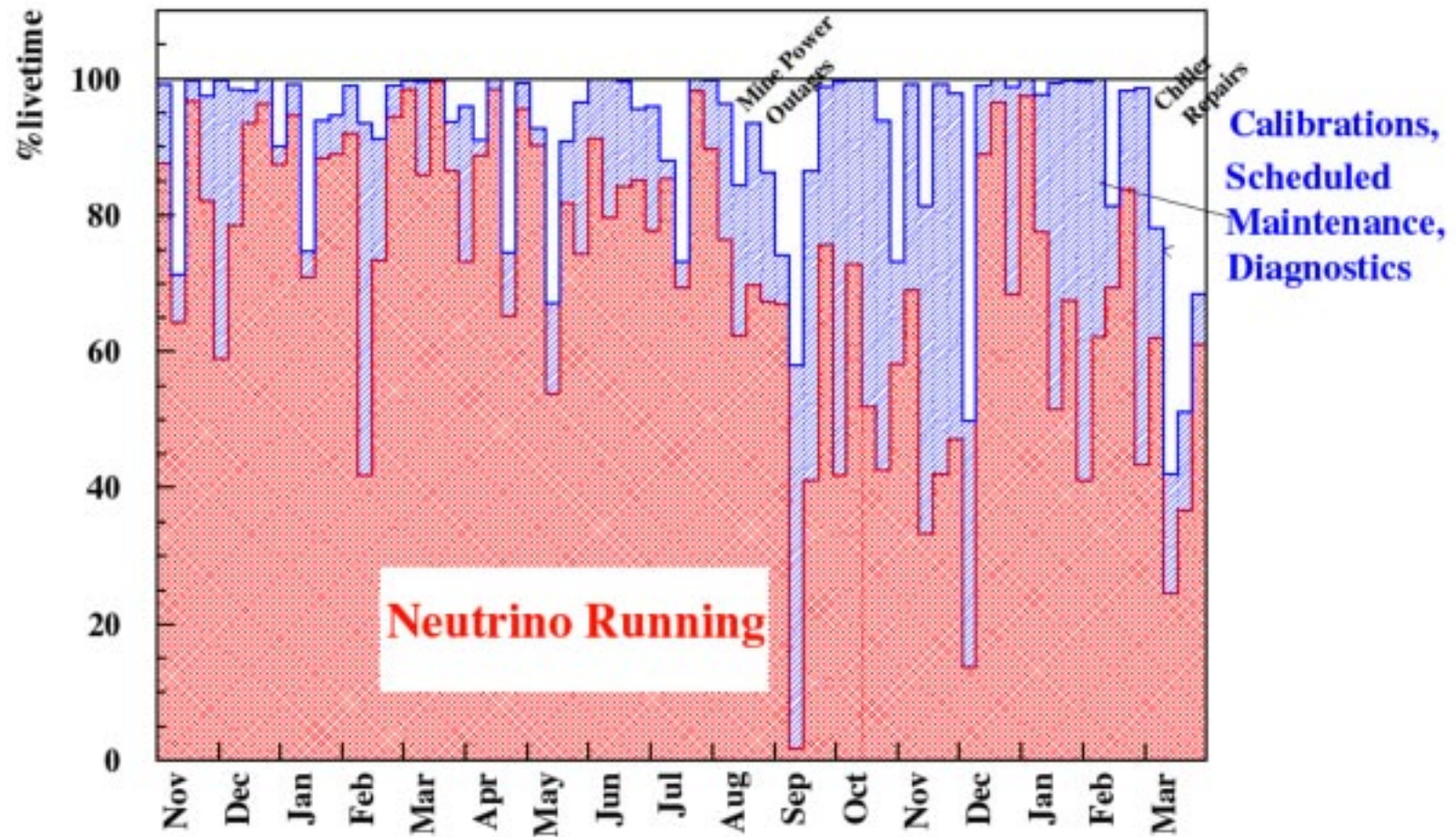
- ☀ (IA) High Threshold & Tight Fiducial Volume for CC & ES Fluxes, Essentially Background Free & with Well-Tested Optics
- ☀ (IB) Low Threshold & Loose Fiducial Volume for NC

II. D20 + SALT

- ☀ Enhanced NC Sensitivity

III. D20 + NCDs

- ☀ Enhanced NC Sensitivity & Event-by-Event Separation of CC & NC



SNO Livetime (Nov. 2, 1999 to Jan. 15, 2001)

240.95 Live Days



- Event Trigger

- Multiplicity Trigger 18 Hit PMTs above 0.25 p.e. Threshold (100% efficiency reached by 23 Hits ~ 3 MeV)
- Total Instantaneous Trigger Rate of 15-18 Hz
- For Each Event Trigger the Charge & Time Response of Each PMT is Recorded
- See NIM A449 (2000) for Electronics & DAQ Details

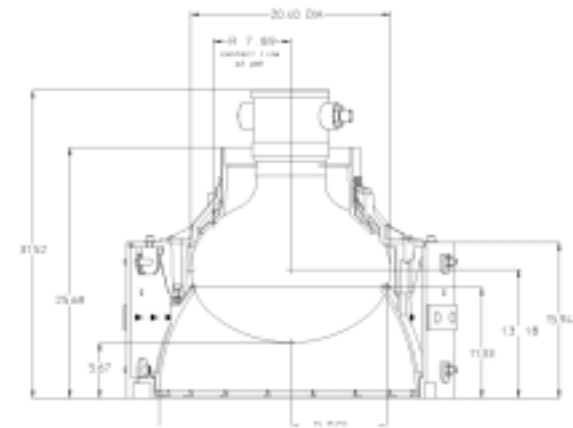
- Data Set

- Data Partitioned into Two Sets
- We Find No Statistically Significant Difference Between the Two Data Sets and Report on the Entire 240.95 Day Sample
 - Establish Data Analysis Procedures on Set-I
 - Blind Test of Bias on Set-II

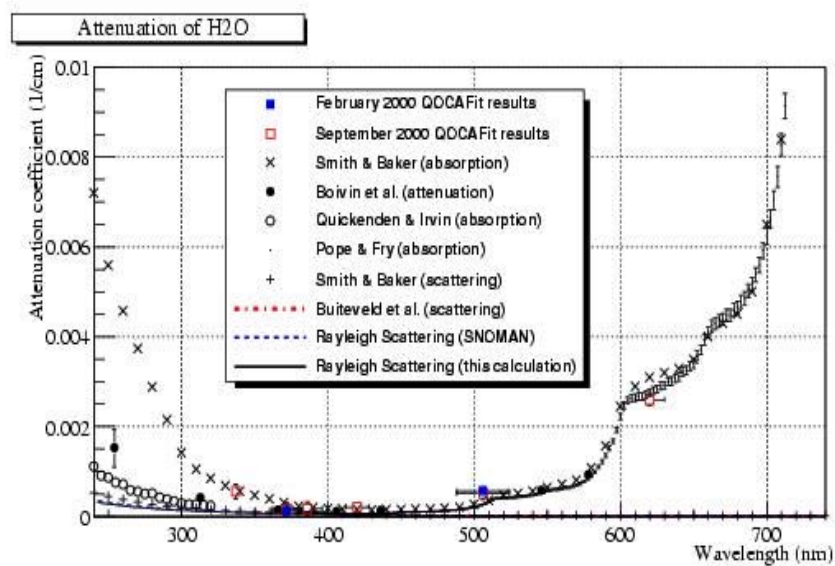
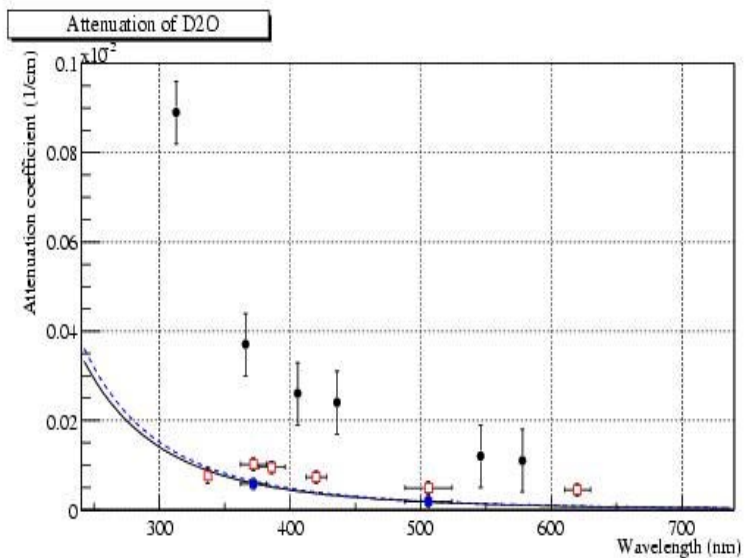
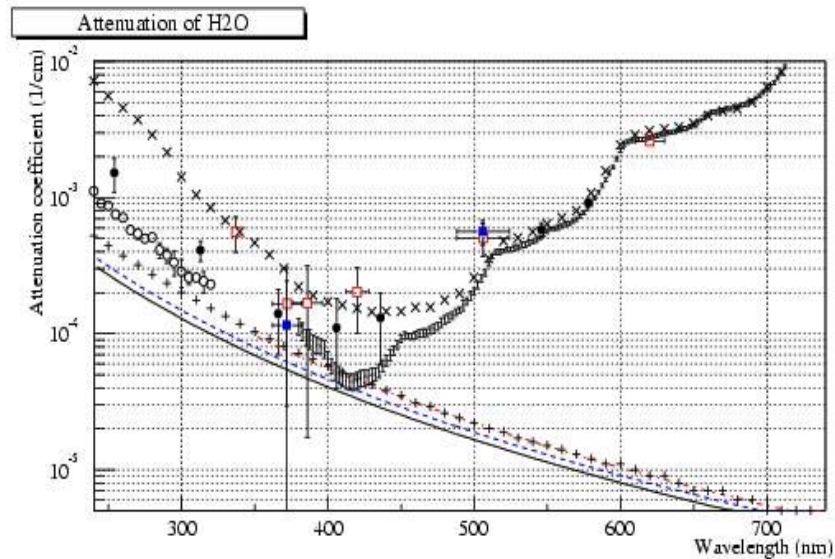
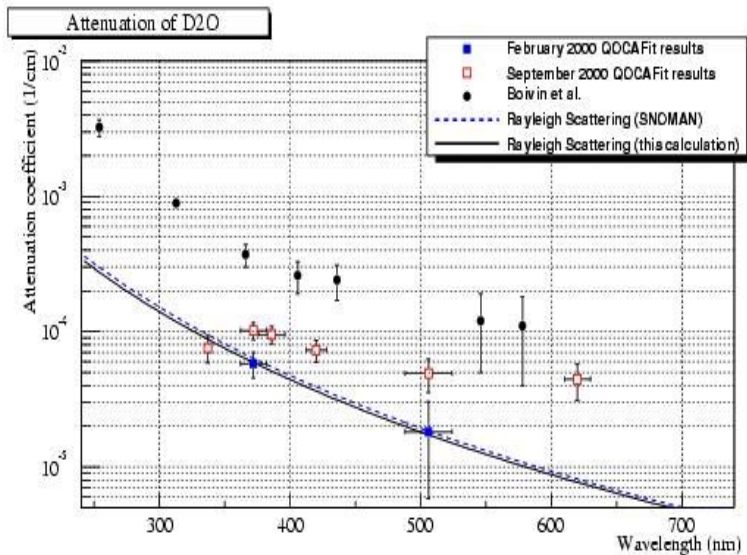
Detector Electronics & Optical Response

- ✱ Characterization with Electronic Pulsers & Pulsed Light Sources
- ✱ Optical Calibration via Diffuse Pulsed Laser Light at 337, 365, 386, 420, 500, and 620 nm

Four Media : D2O
Acrylic Vessel
H2O
PMT Response



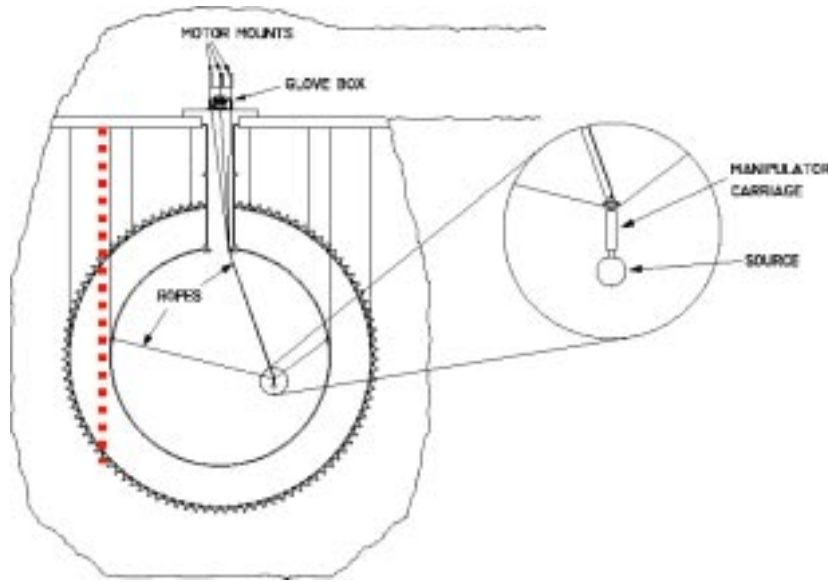
- ✱ Attenuation, Reflection, Scattering, Geometry ... Effects on Event Reconstruction and Energy Response as Function of Position



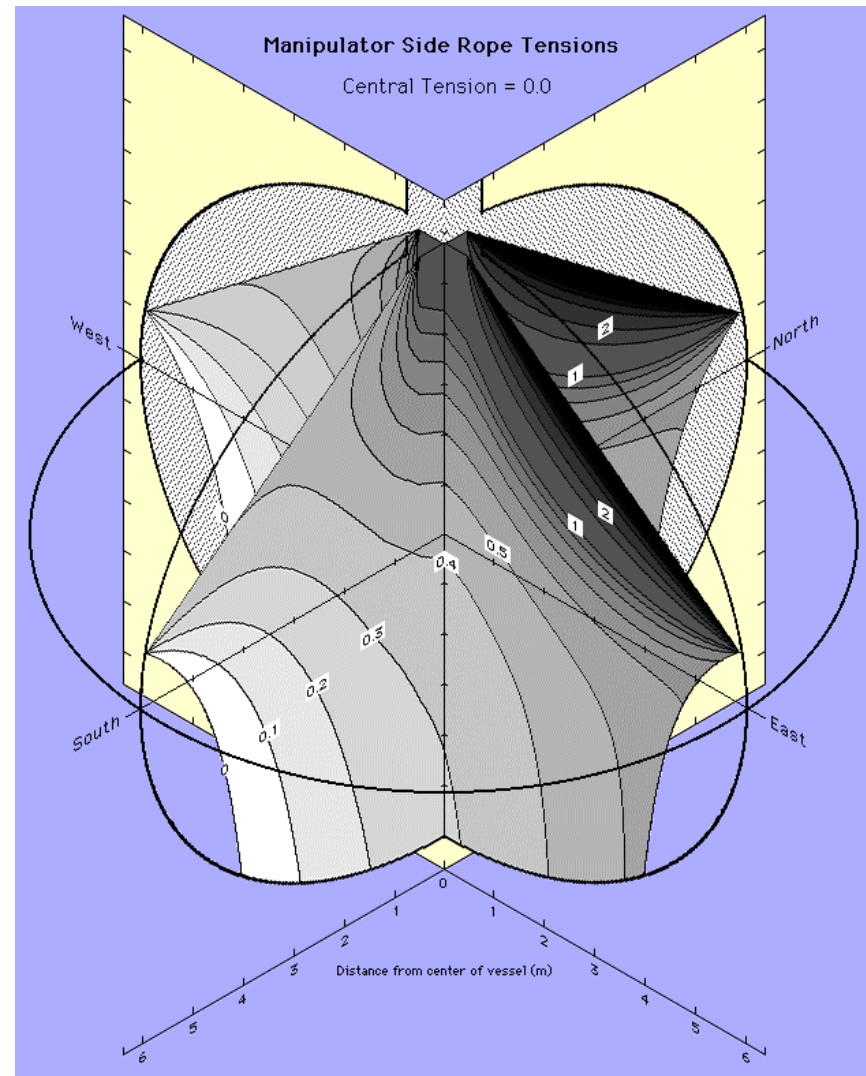
Energy Response

- ★ Absolute Energy Scale via Triggered ^{16}N (6.13 MeV Gamma) Deployed over Two Planar Grids in D_2O & Linear Grid in H_2O to Determine Position & Direction Dependence of Energy Response
- ★ ^8Li Beta Decay Electrons & pT Generated 19.8 MeV Gamma
- ★ ^{252}Cf Neutrons (6.25 MeV Capture Gamma) Provide Extended Distribution for Further Test of Spatial Dependency & Expt'l Determination of Neutron Capture Efficiency

Calibration Systems

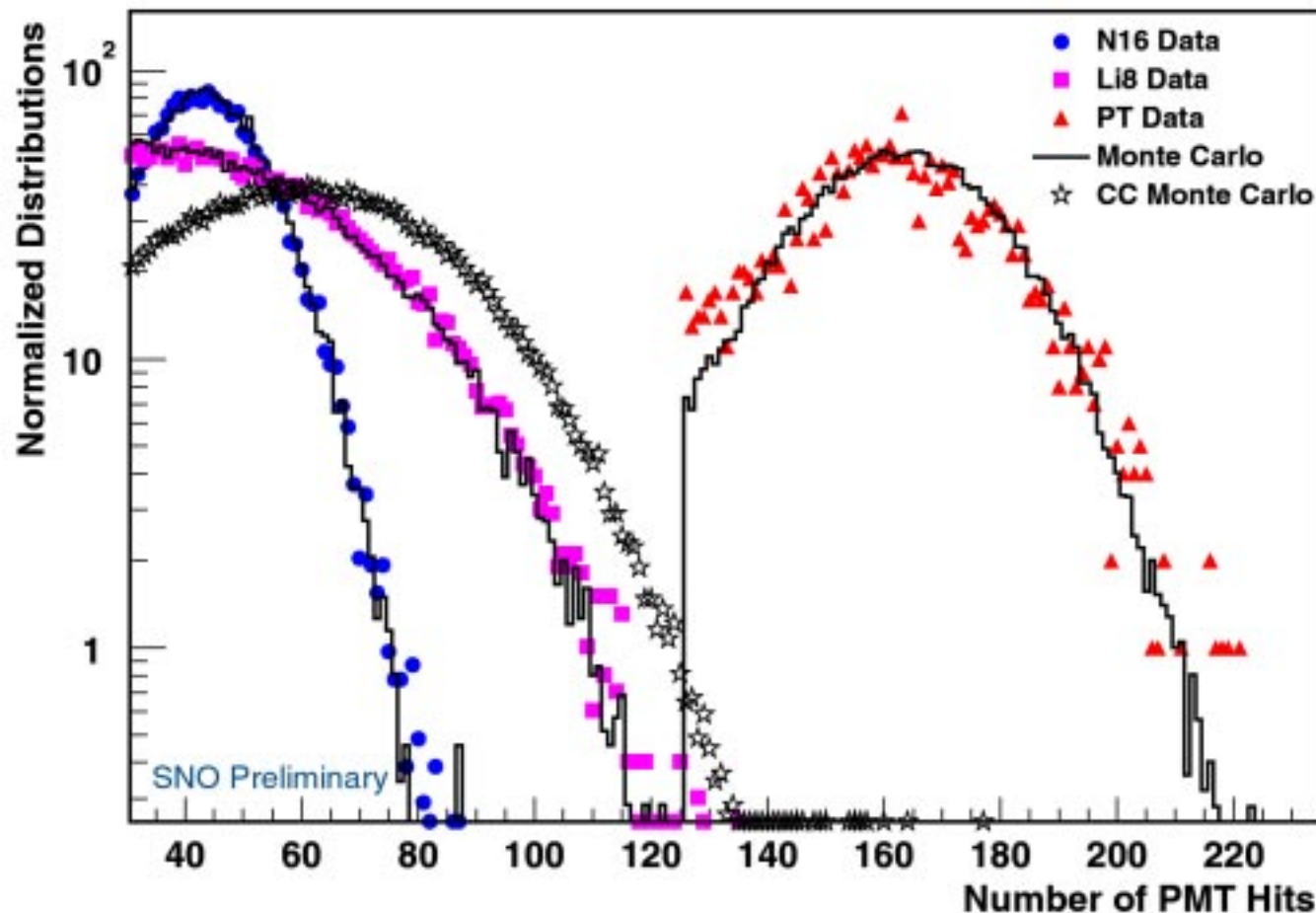


- Deploy Sources
 - In two Planes in D_2O
 - On one line in H_2O

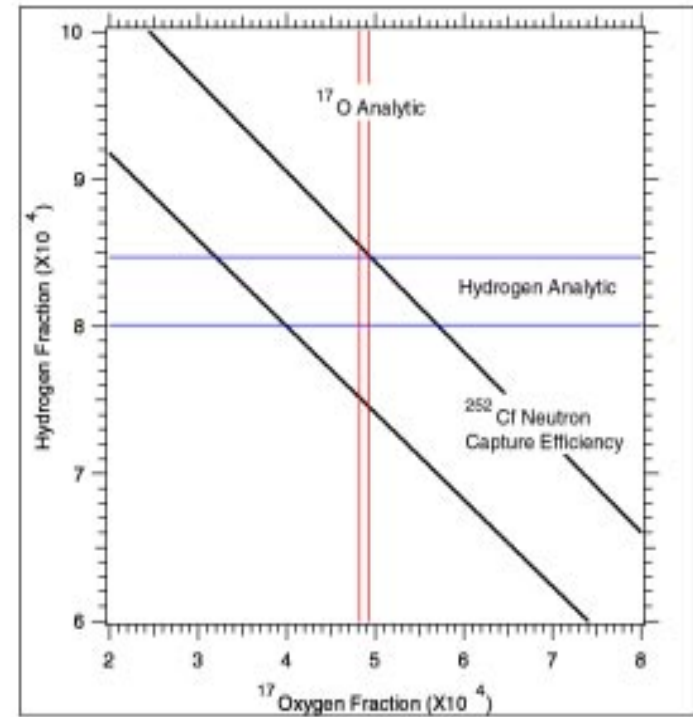
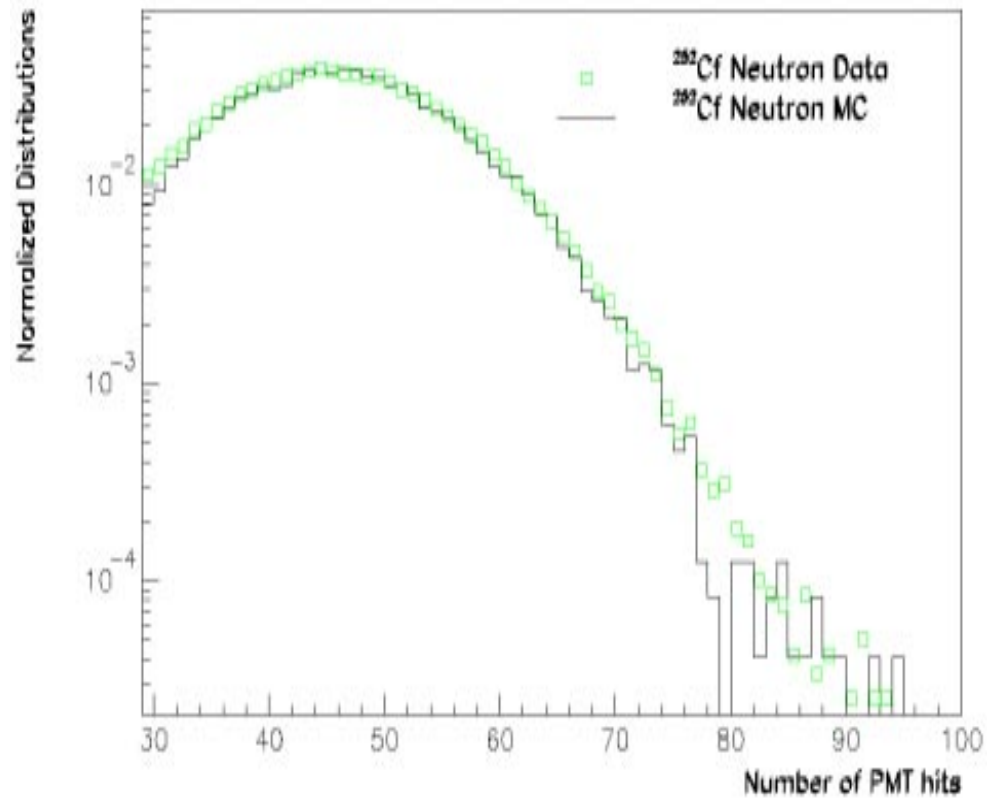


SNO's Energy Response

Energy Response at the Center of the Detector



Calibration with Neutrons

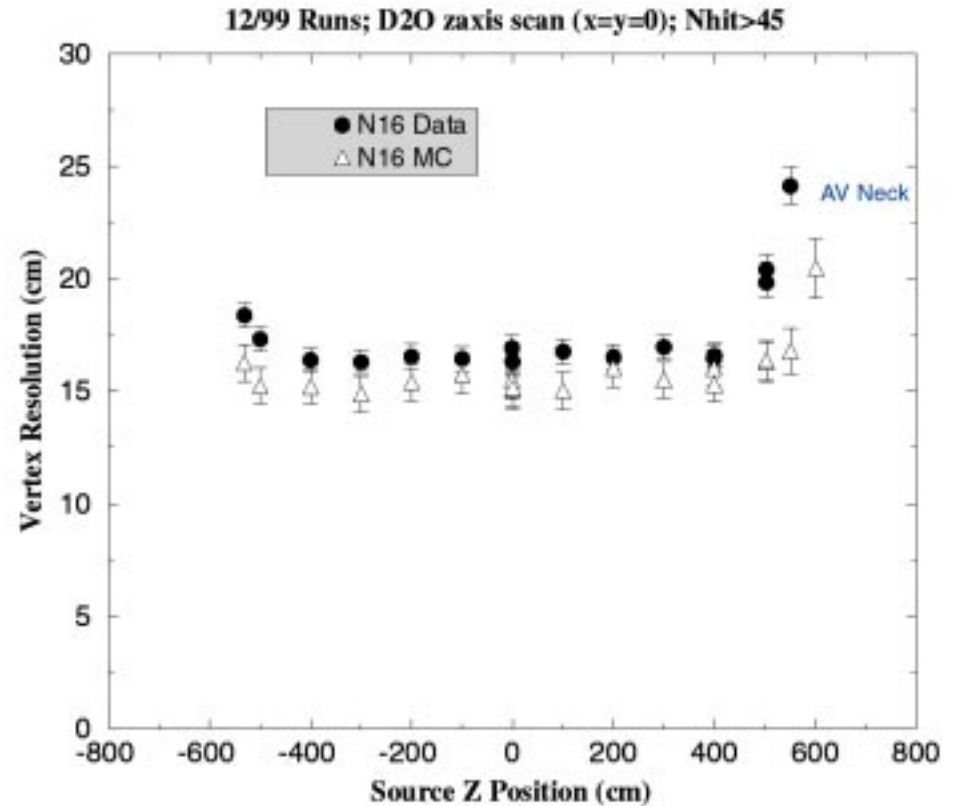
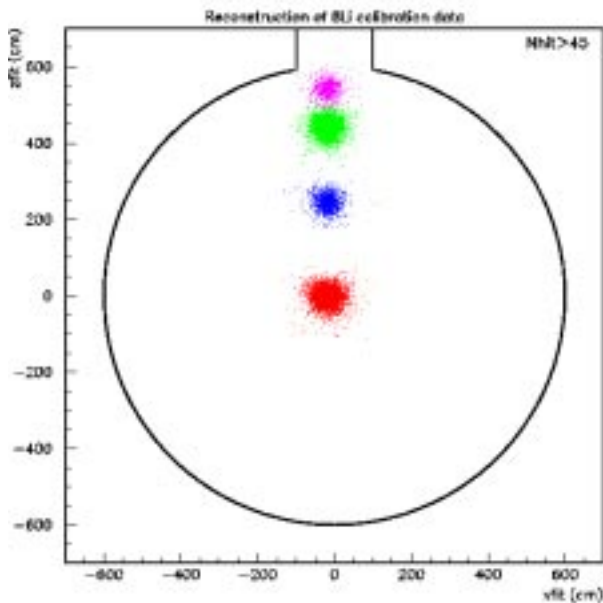


Detector Resolution

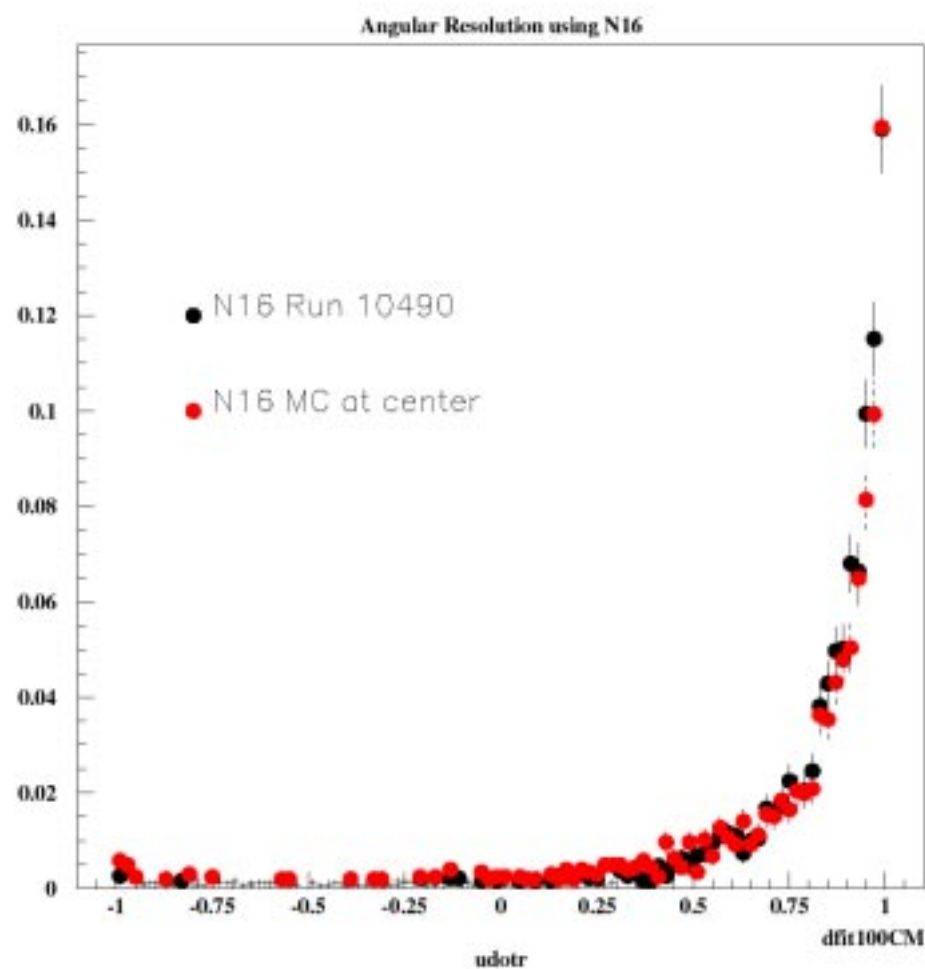
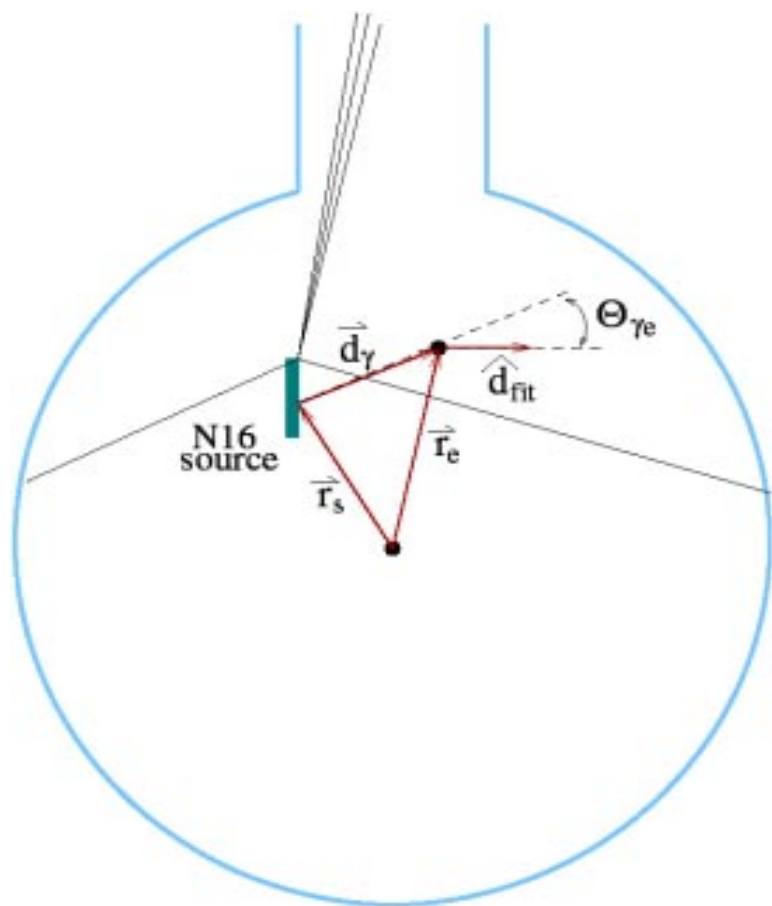
- ✱ Position, Angular & Energy Resolution Established with Cerenkov Light Sources
- ✱ Exploit Calibrated Time & PMT Position Distribution to Reconstruct Vertex Position & Direction of Event
- ✱ Position Resolution (16 cm) via Electrons from ^8Li Beta Decay & Compton Electrons from ^{16}N
- ✱ Angular Resolution(13.5 Degrees) via ^{16}N Gamma Rays that Produce Compton Electrons that Reconstruct more than 150 cm From Source

Event Reconstruction

- Calibrated with ^{16}N γ 's & ^8Li β 's throughout D_2O ^{16}N γ 's in H_2O



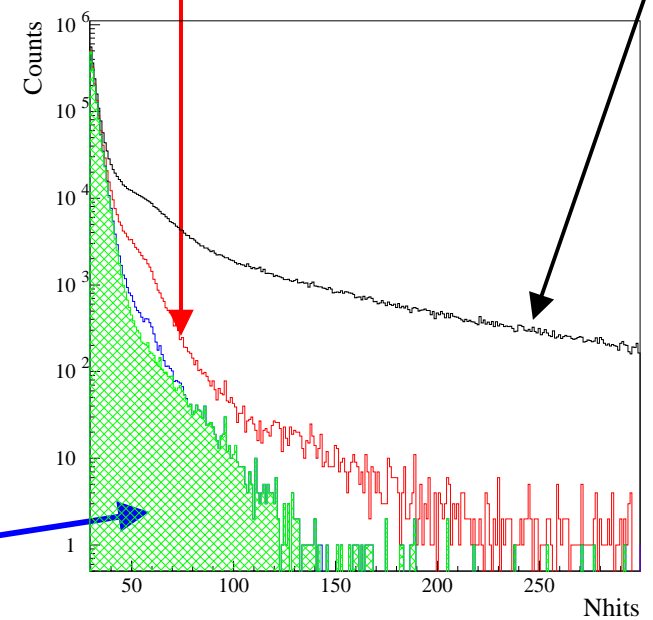
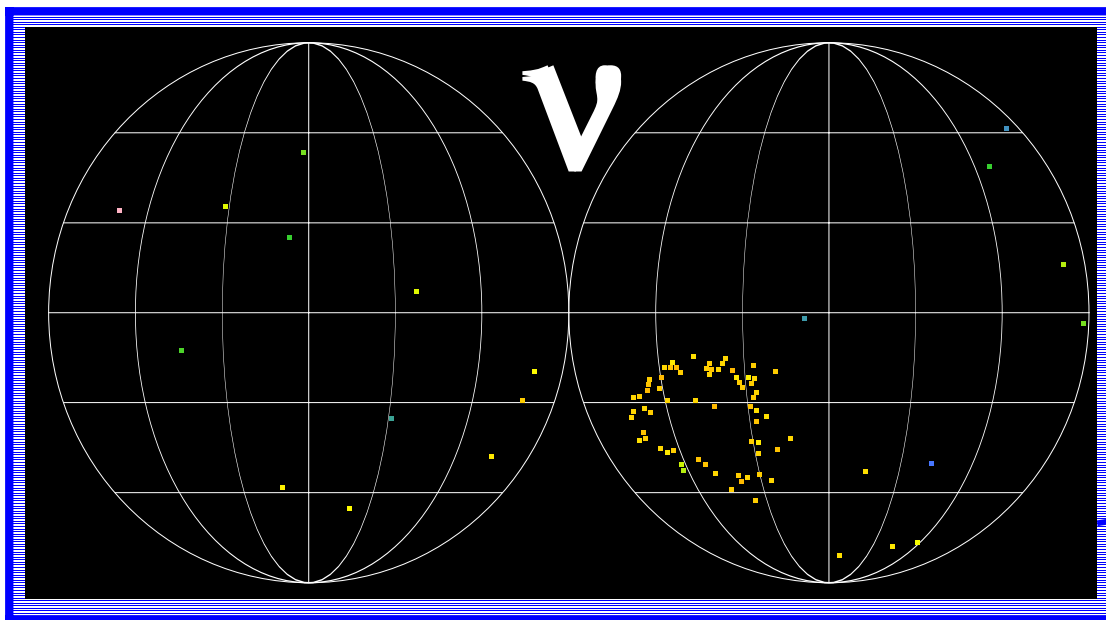
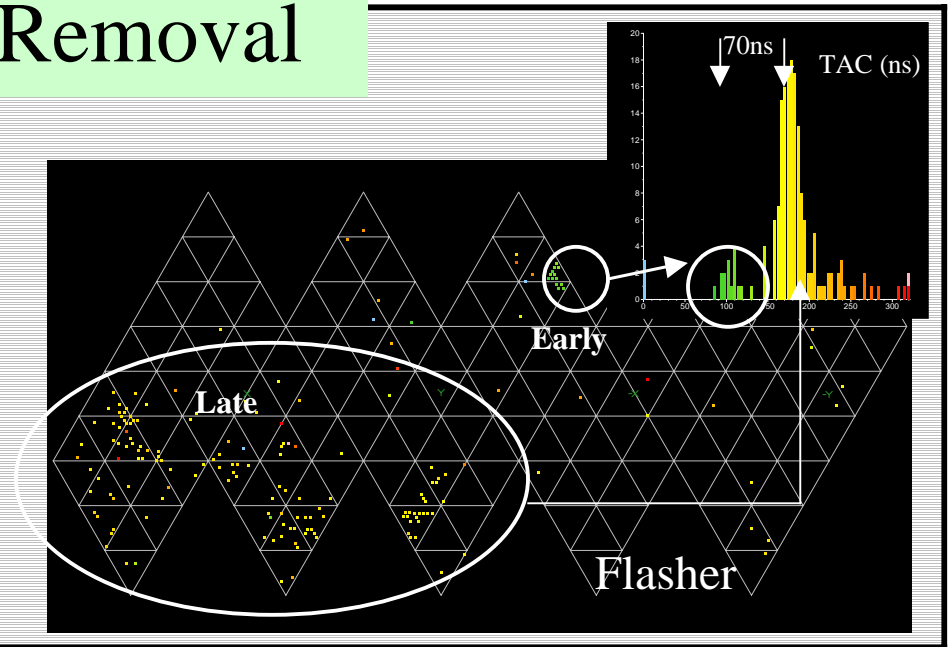
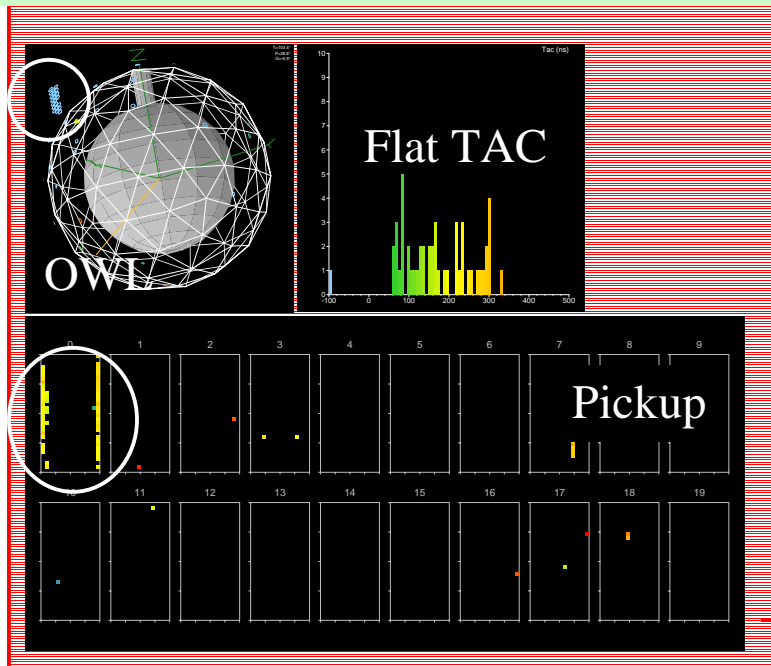
Angular Resolution



Data Reduction - Instrumental Backgrounds

- ★ Light Pulses Associated with Electrical Discharge from PMTs, Insulating Materials in Water Circulation Hardware, Insulators Exposed in the Neck of the AV, and Electrical Pick-UP
- ★ Instrumental Background Events have Characteristics Very Different than Cerenkov Light and are Eliminated Using Cuts Based on PMT Position, Calibrated PMT Time & Charge, Event-To-Event Time Correlations, and Veto-Tubes.
- ★ Instrumental Background Removal is Verified by Comparing Results from Two Independent Background Rejection Analyses

Instrumental Background Removal



Higher Level Data Cuts

Discriminates between single Cerenkov e^- and multiple vertices

- Based on In-Time Light (ITR)
- Average Angle between hit PMTs (Θ_{ij})

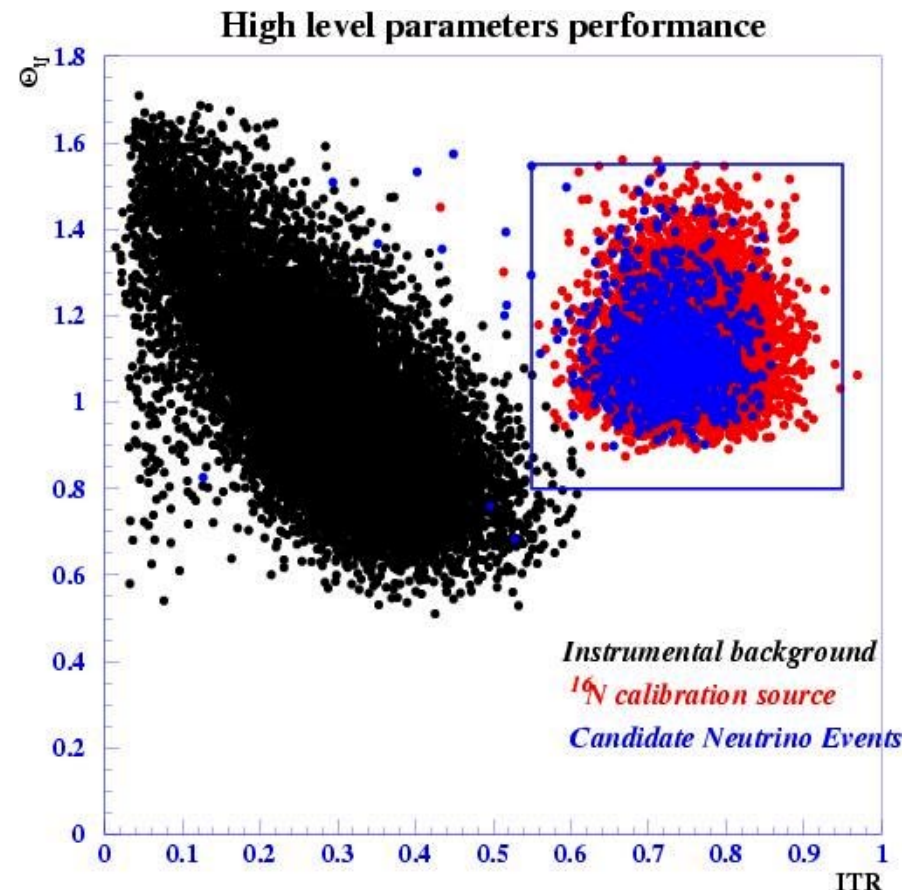
Volume Weighted Signal Loss

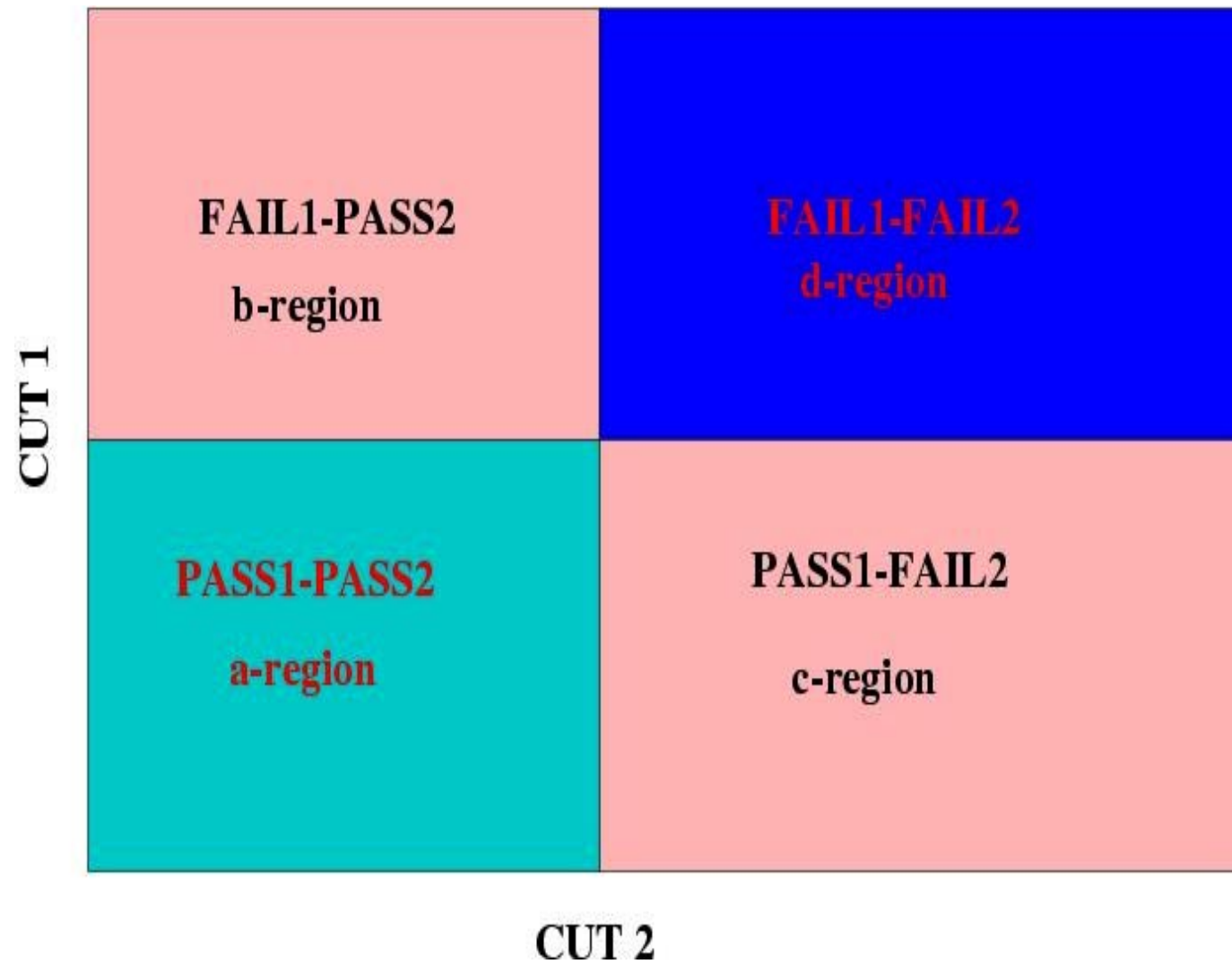
$1.38^{+0.7}_{-0.6} \%$

Contamination

(Bifurcated Analysis and Handscanning)

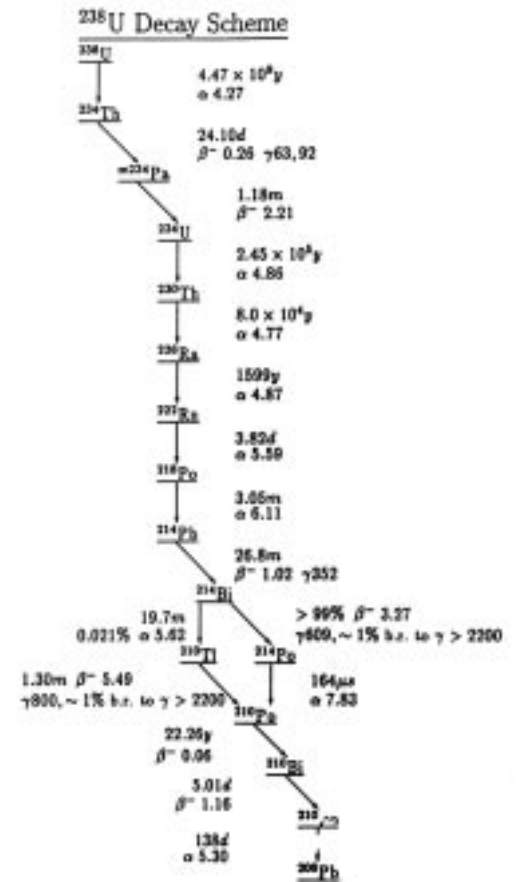
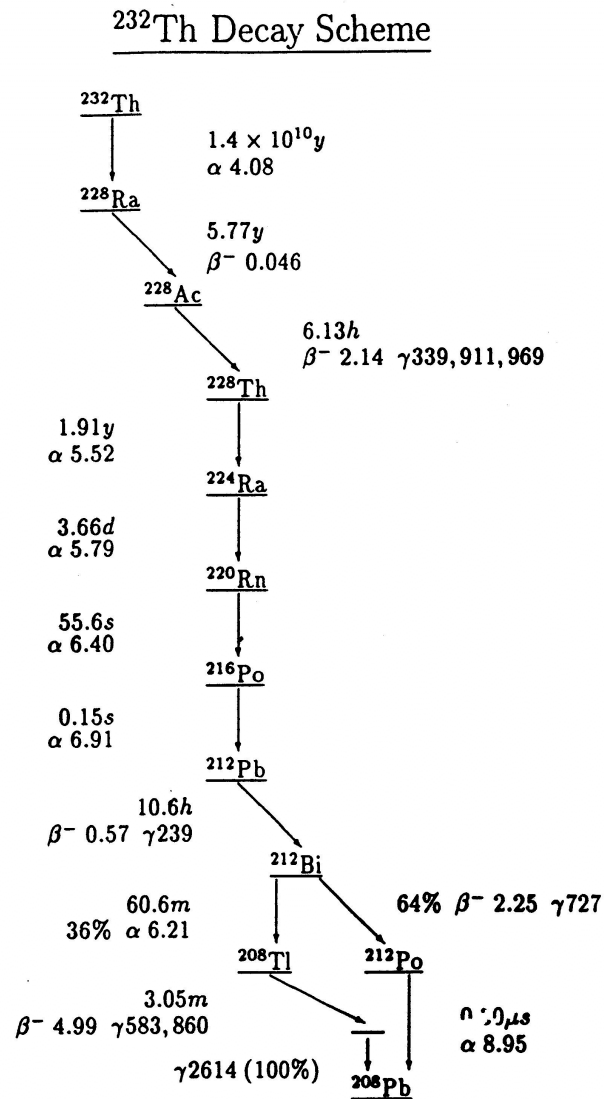
$< 0.2 \%$



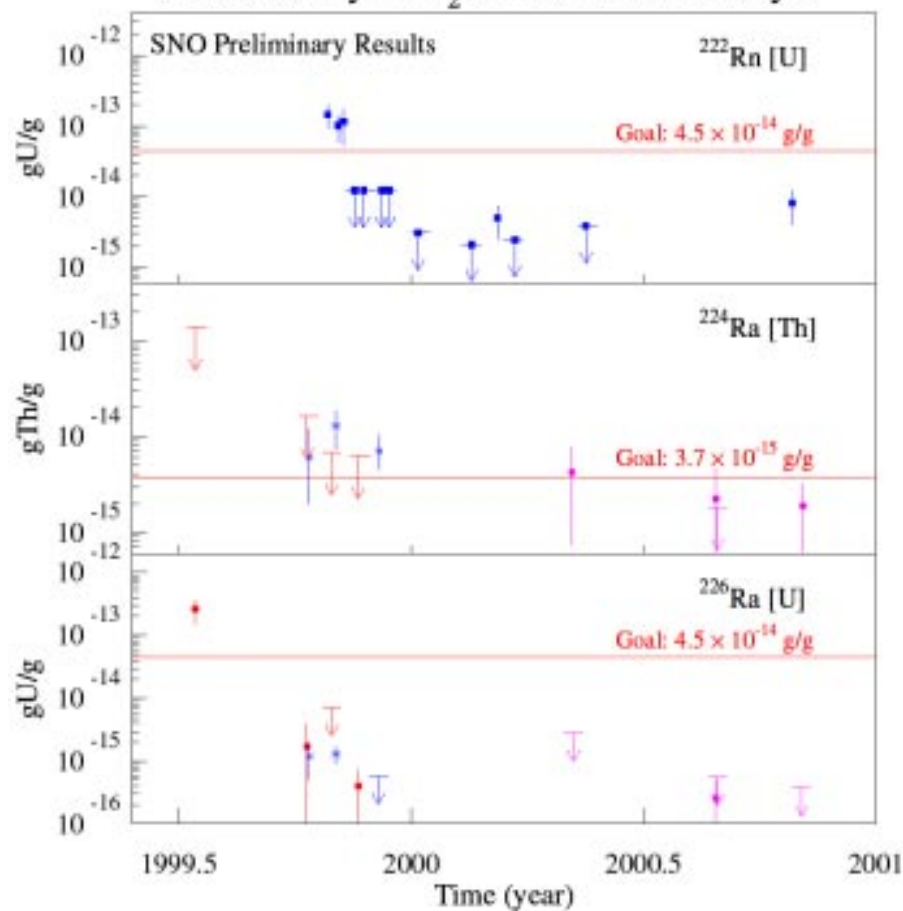


Radioactive (Physics) Background

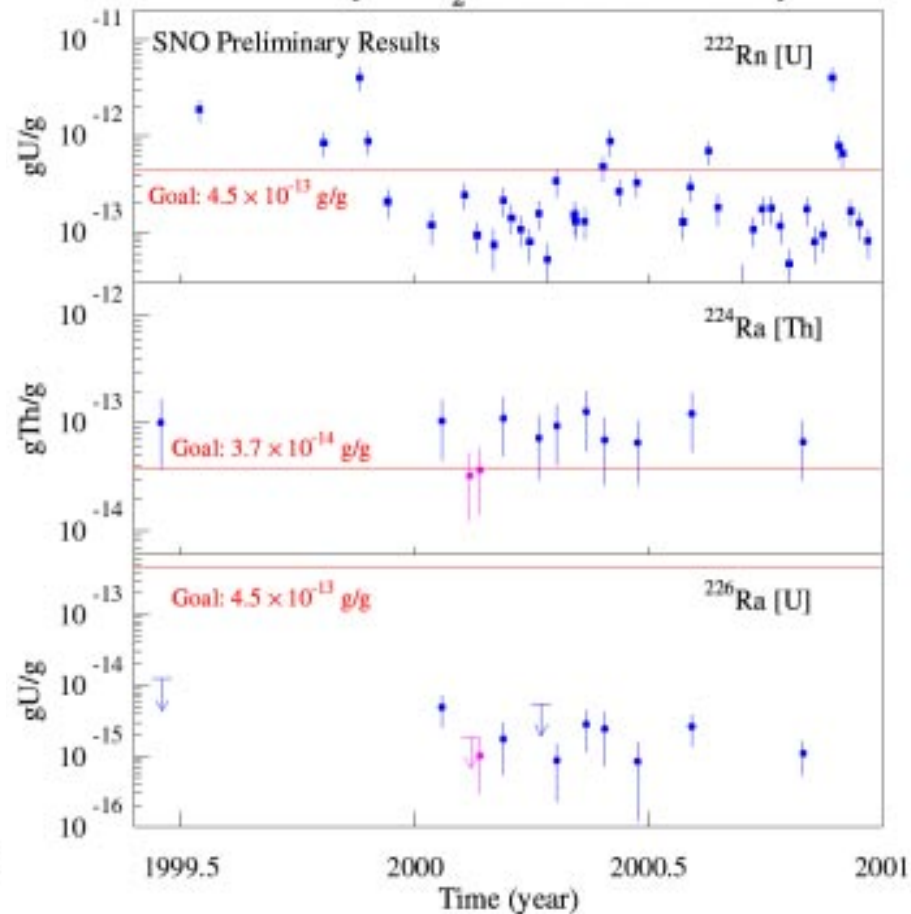
- ☀ D₂O U & Th
- ☀ AV U & Th
- ☀ H₂O U & Th
- ☀ PMT β - γ
- ☀ High Energy γ 's



Radioactivity in D₂O from Water Assays

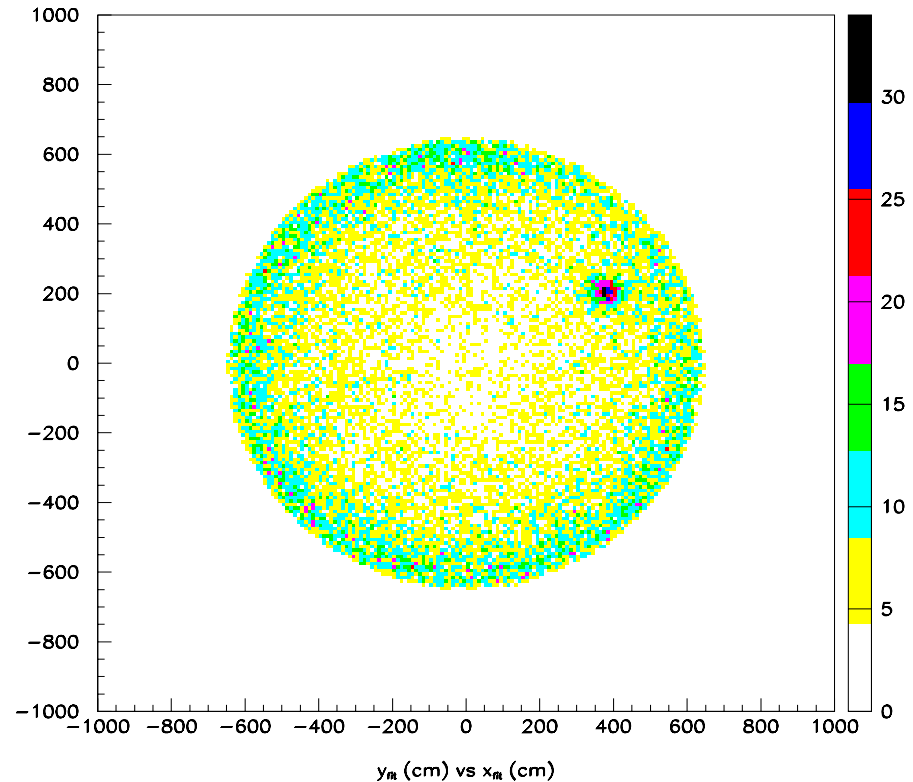


Radioactivity in H₂O from Water Assays



Acrylic Vessel Backgrounds

- Direct Counting and NAA
- Encapsulated U, Th sources
- Direct Observation in Cerenkov Light



- Small Neutron background

☞ Activities assayed to be
<10% Targets ~0.2 ppt

☞ “Berkeley Blob”
 $\sim 9^{+20}_{-5} \pm 3 \mu\text{g}$ ‘Th’

Data Analysis

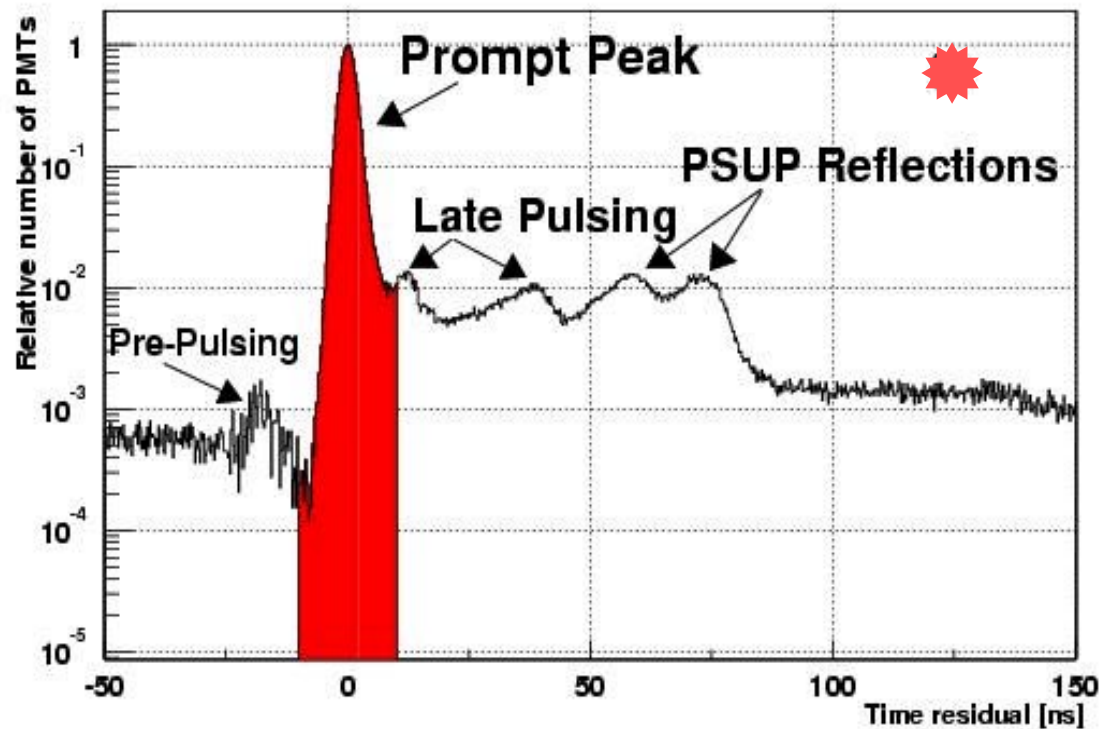
- Components

- Removal of Instrumental BGND
- Event Reconstruction
- High Level Cuts
- Determine Physics BGND
- Decomposition of Signals in Components
- Error and Systematics Estimation

- Verification

- Blind Data Set
- Develop and Maintain Independent and Redundant Analysis Components

- ✱ For Each Event in the D2O Volume an Effective Kinetic Energy Estimator is Calculated Using Prompt (Un-Scattered) Cerenkov Photons and the Reconstructed Position & Direction of the Event



- ✱ Verification with a Second Energy Estimator using ALL Light Within 93 ns and Without Position & Direction Corrections

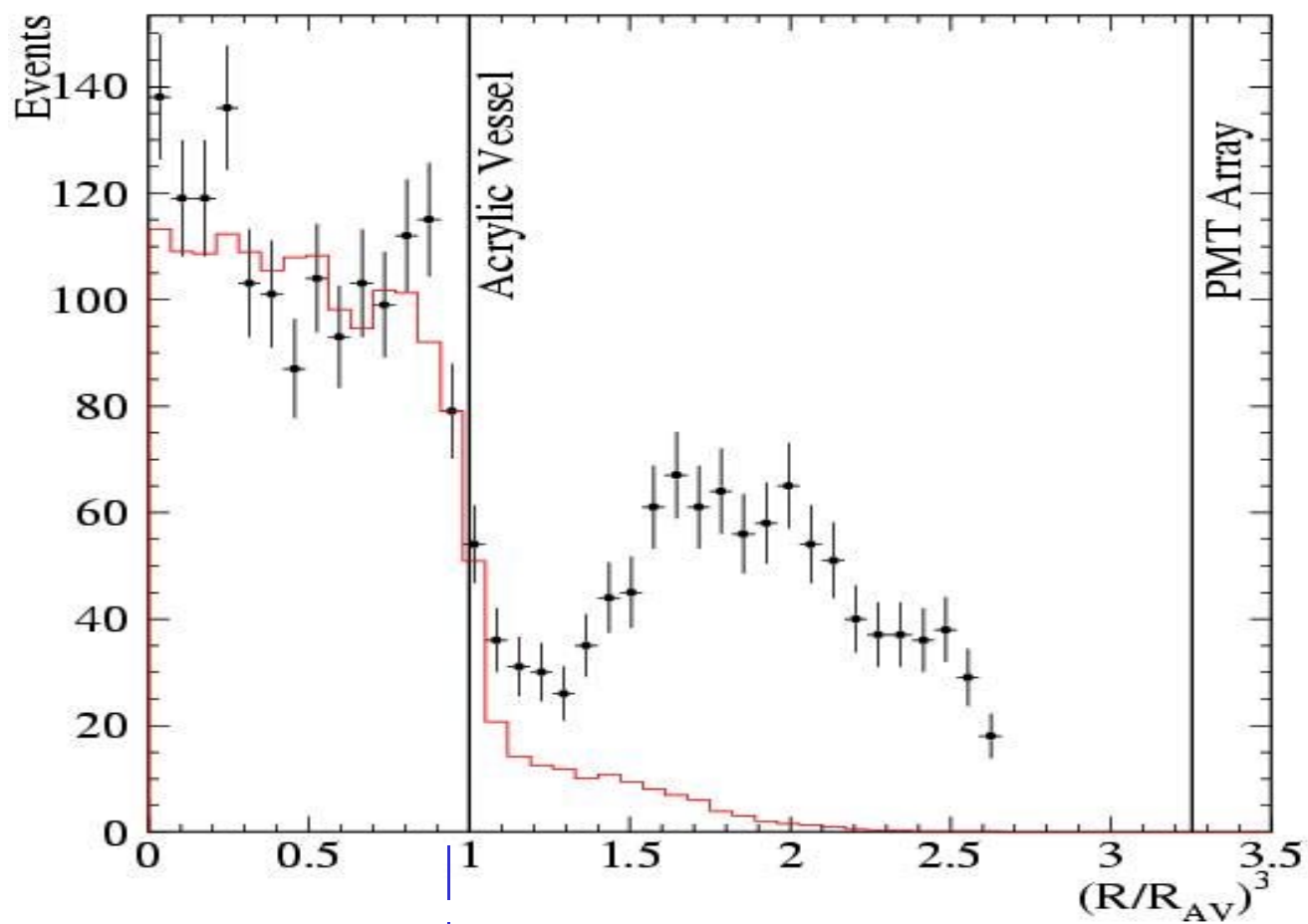
☀ We Restrict Our Kinetic Energy Threshold to 6.75 MeV in order to Minimize Tails from Low Energy Background and Neutron Capture on Deuterium

☀ We Restrict our Fiducial Volume to Events Reconstructed within 550 cm in order to Minimize Background Tails & to rely upon Well-Tested Optics & Calibration

☀ Signals are Decomposed by Fitting the Data Distributions to Probability Distribution Functions Characterized by $\{E, R^3, \text{Cos}\theta_{\text{Sun}}\}$

☀ Verification of Signal Decomposition using N_Hit Estimator with Different Choices of Threshold & Fiducial Volume with Background Characterized by PDFs.

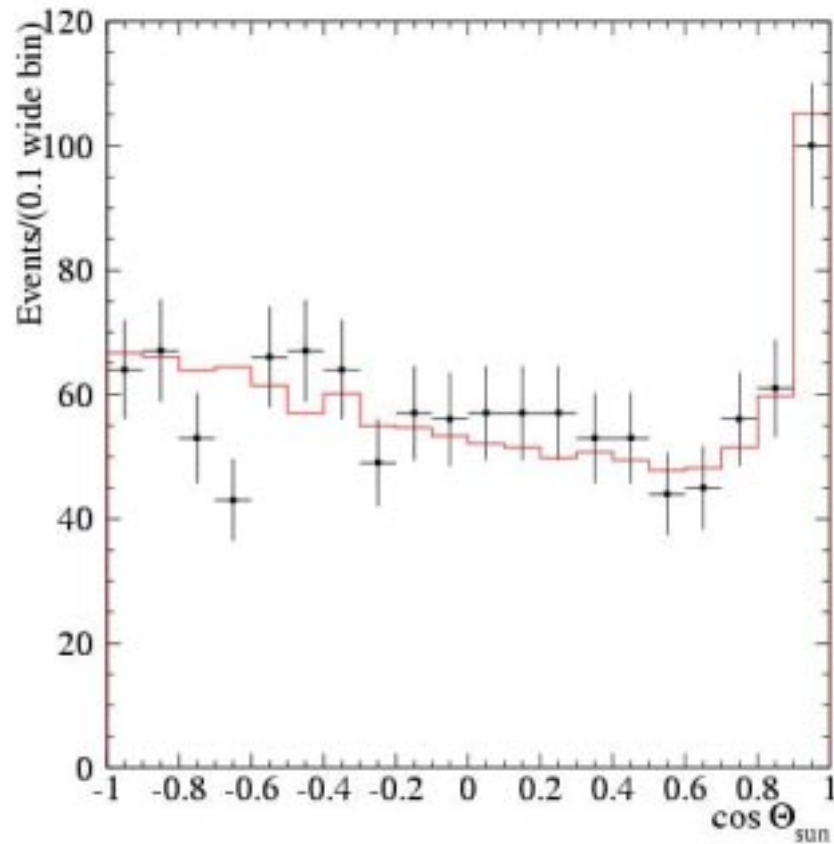
Radial Distribution ($E > 6.75$ MeV)



<--- Fiducial Volume Cut at 550 cm

Angular Distribution

(Direction of Events with respect to the SUN)



ES Component Forward Peak

CC Component $\sim 1 - 0.3 \cos \Theta_{\text{sun}}$

Neutrons & Bgnds Flat

Data Flow Table

Analysis Step	
Total event triggers	Number of Events
Neutrino data triggers	355,320,964
$N_{\text{hits}} \geq 30$	143,756,178
Instrumental background cuts	6,372,899
Muon followers	1,842,491
High level cuts	1,809,979
Fiducial volume cut	956,535
Threshold cut	18,783
Total Events	1,169

Extended ML Decomposition of Signal

- ★ The Final Data Sample Contains 1169 Events after Energy Threshold & Fiducial Volume Cuts

$$\Rightarrow \left\{ \begin{array}{l} \text{CC} = 975.4 \pm 39.7 \text{ events} \\ \text{ES} = 106.1 \pm 15.2 \text{ events} \\ \text{neutrons} = 87.5 \pm 24.7 \text{ events} \end{array} \right.$$




Results for Solar Neutrino Fluxes

In units of 10^6 Neutrinos $\text{cm}^{-2} \text{s}^{-1}$

$$\phi_{\text{CC}}^{\text{SNO}} = 1.75 \pm 0.07 \pm 0.12 \pm 0.05 = 1.75 \pm 0.15$$

$$\phi_{\text{ES}}^{\text{SNO}} = 2.39 \pm 0.34 \pm 0.16 = 2.39 \pm 0.38$$

$$\phi_{\text{ES}}^{\text{SK}} = 2.32 \pm 0.03 \pm 0.08 = 2.32 \pm 0.09$$

  
Stat. Sys. X-Sect.

Systematic Errors for Fluxes

Error Source	CC error (%)	ES error (%)
Energy scale	-5.2, +6.1	-3.5, +5.4
Energy resolution	± 0.5	± 0.3
Non-linearity	± 0.5	± 0.4
Vertex shift	± 3.1	± 3.3
Vertex resolution	± 0.7	± 0.4
Angular resolution	± 0.5	± 2.2
High Energy γ 's	-0.3, +0.0	-1.8, +0.0
Low energy background	0.0	0.0
Instrumental background	-0.2, +0.0	-0.5, +0.0
Trigger efficiency	0.0	0.0
Live time	± 0.1	± 0.1
Cut acceptance	-0.6, +0.7	-0.6, +0.7
Earth orbit eccentricity	± 0.2	± 0.2
^{17}O , ^{18}O	0.0	0.0
Experimental uncertainty	-6.2, +7.0	-5.7, +6.8
Cross-section	3.0	0.5
Solar Model	-16, +20	-16, +20

Interpretation of Fluxes in terms of Active Neutrino Oscillations

In units of 10^6 Neutrinos $\text{cm}^{-2} \text{ s}^{-1}$

$$\phi_{\text{CC}}^{\text{SNO}} = \phi_e = 1.75 \pm 0.07 \pm 0.12 \pm 0.05 = 1.75 \pm 0.15$$

$$\phi_{\text{ES}}^{\text{SNO}} = \phi_e + \epsilon \phi_{\mu\tau} = 2.39 \pm 0.34 \pm 0.16 = 2.39 \pm 0.38$$

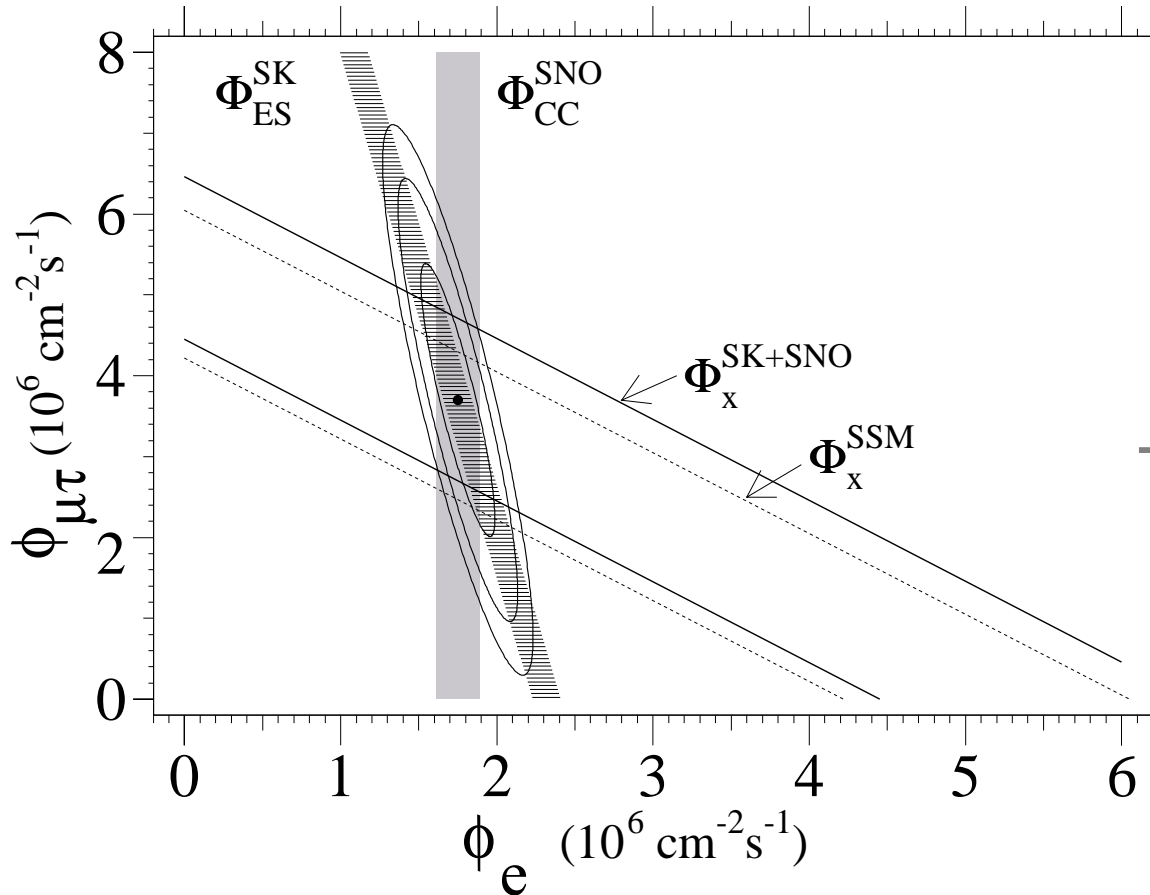
$$\phi_{\text{ES}}^{\text{SK}} = \phi_e + \epsilon \phi_{\mu\tau} = 2.32 \pm 0.03 \pm 0.08 = 2.32 \pm 0.09$$

$$\epsilon \phi_{\mu\tau} = \phi_{\text{ES}}^{\text{SK}} - \phi_{\text{CC}}^{\text{SNO}} = 0.57 \pm 0.17 \text{ (3.3 } \sigma \text{)}$$

$$\phi_{\mu\tau} = 3.69 \pm 1.13 \text{ (3.3 } \sigma \text{)}$$

- ★ The probability that the SNO result is not a downward fluctuation from the SK result is 99.96%.

Flavor Content of the 8B Solar Neutrino Flux



Gives total ^8B Flux of
 $5.44 \pm 0.99 \times 10^6 \text{ cm}^{-2} \text{ s}^{-1}$

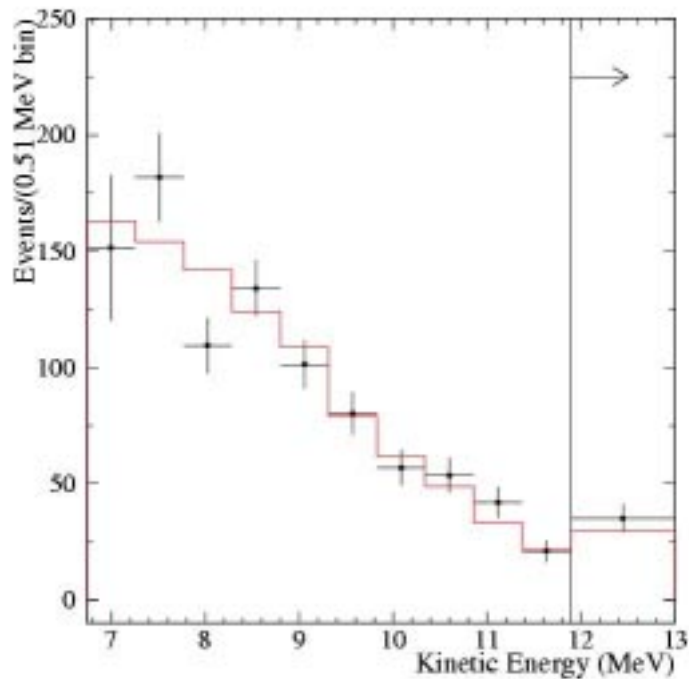
Note: this is in excellent
 agreement with the BP2001
 prediction of $5.05^{+1.01}_{-0.81}$

The CC result from SNO combined with the ES result from SK give dramatic evidence for the oscillation of electron neutrinos to muon and/or tauneutrinos!!!!

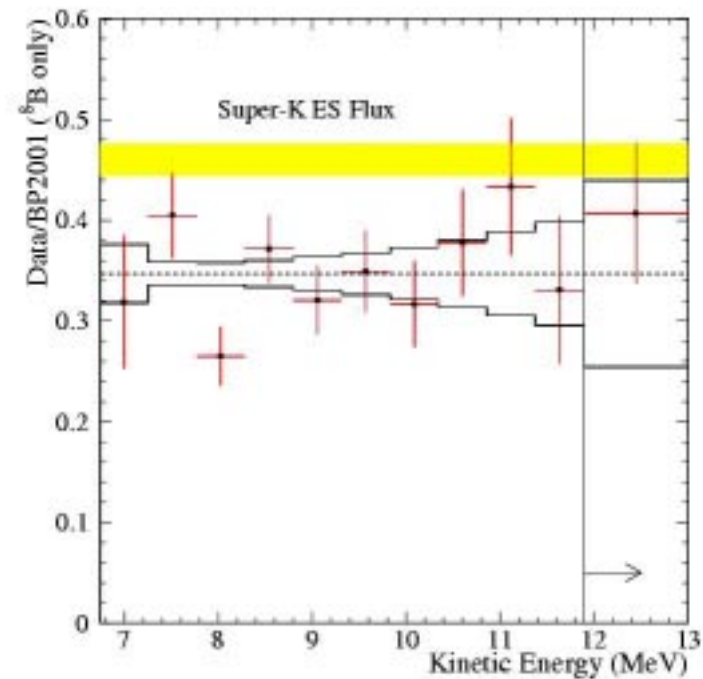
So it Appears that the Sun Does Shine as Brightly Underground ...

As on the Surface!

Charged Current Energy Spectrum



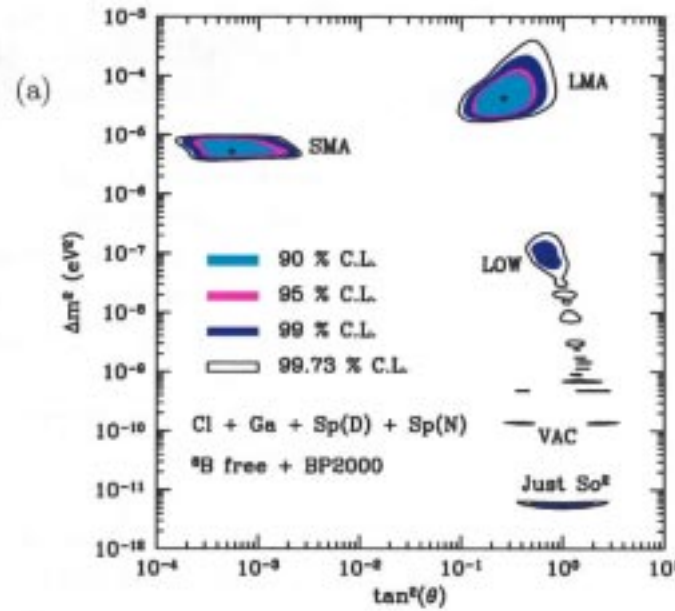
CC spectrum derived from fit
without constraint on shape
of ^8B spectrum



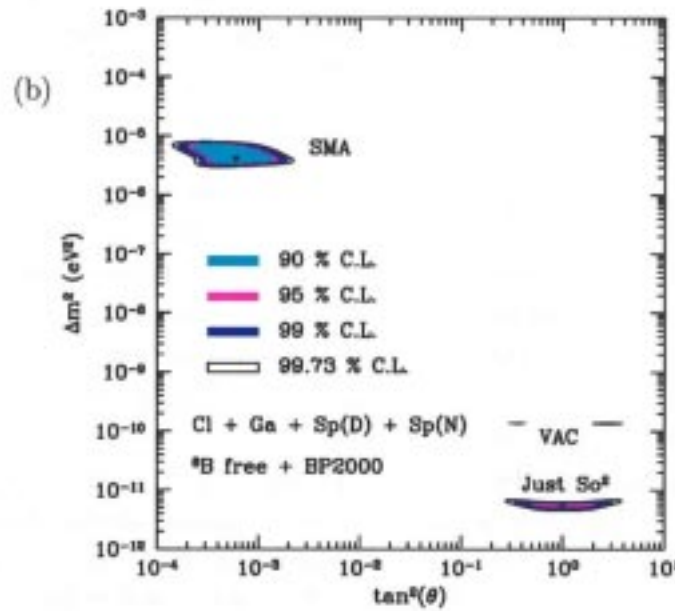
CC spectrum normalized to
predicted ^8B spectrum.
No evidence for shape
distortion.

Pre-SNO Oscillation Solutions

Bahcall, Krastev, Smirnov



Active



Sterile

Constraints on Oscillation Scenarios ?

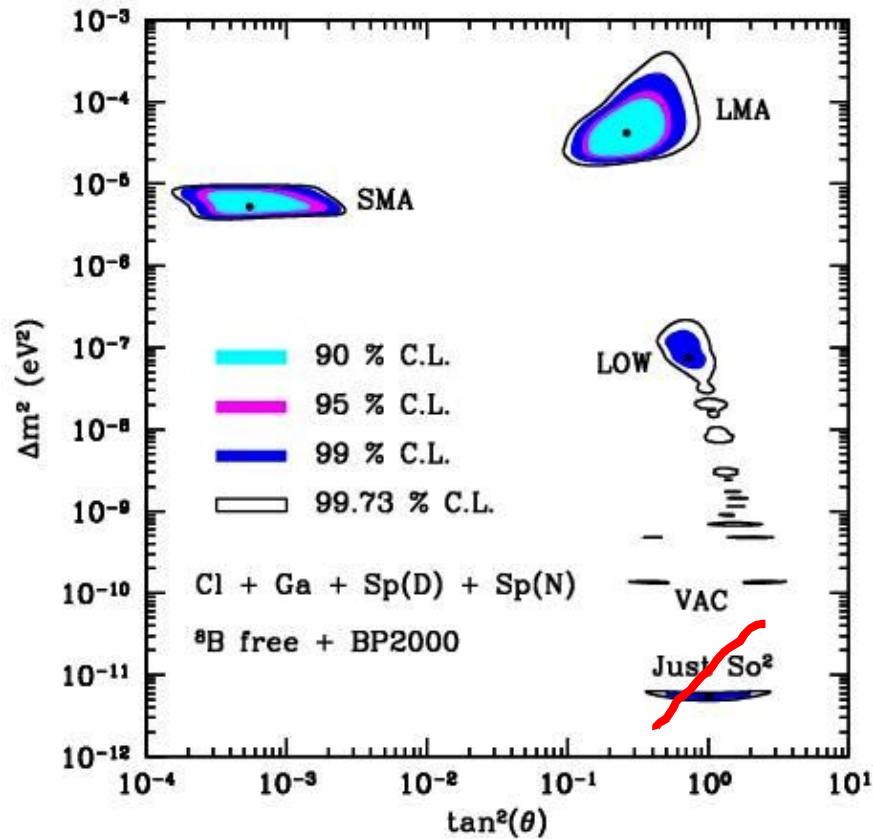
These data exclude the Just-So² parameters for neutrino oscillation recently identified at $\Delta m^2 = 6 \times 10^{-12} \text{ eV}^2$.

SMA sterile neutrinos are also excluded.

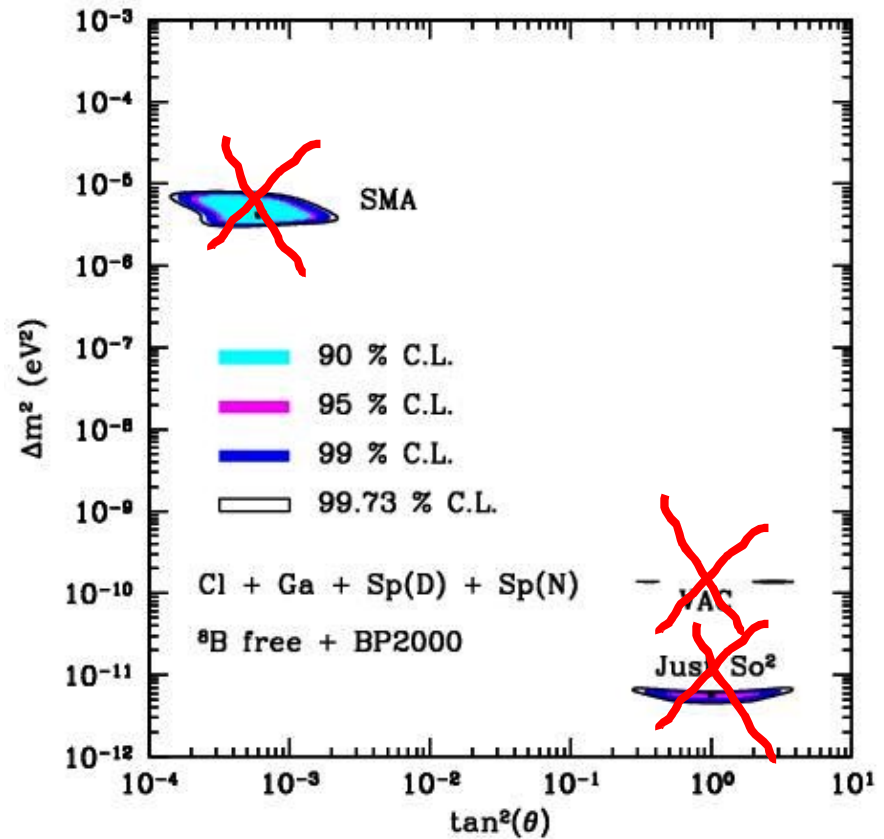
If oscillation with maximal mixing to a sterile neutrino is occurring the SNO CC-derived ⁸B flux above a threshold of 6.75 MeV will be essentially identical with the integrated Super-Kamiokande ES-derived ⁸B flux above a threshold of 8.5 MeV. Correcting for the ES threshold the flux difference is 0.53 ± 0.17 , or $3.1 \sigma \rightarrow$ excludes the sterile vacuum solution.

These data rule out oscillations to Sterile neutrinos and exclude the “Just so²” parameters.

Post-SNO IA Solutions for Neutrino Oscillations



Active Neutrinos



Sterile Neutrinos

Summary & Conclusions

- ☺ The SNO detector is taking beautiful data. Phase IA is complete!
- ☺ The CC rate is low compared to the SSM prediction, and to the ES rates as measured by SNO and SK. This provides strong evidence for ν_e oscillations.
- ☺ The Just So^2 and sterile neutrino parameter spaces are excluded. Oscillation is to active neutrinos.
- ☺ These results provide the first direct evidence of active neutrinos other than ν_e in the solar neutrino flux.
- ☺ The total flux of active ^8B neutrinos agrees well with the SSM predictions.

The Three Phases of SNO

I. Pure-D20

- ☀ (IA) High Threshold & Tight Fiducial Volume for CC & ES Fluxes, Essentially Background Free & with Well-Tested Optics
- ☀ (IB) Low Threshold & Loose Fiducial Volume for NC

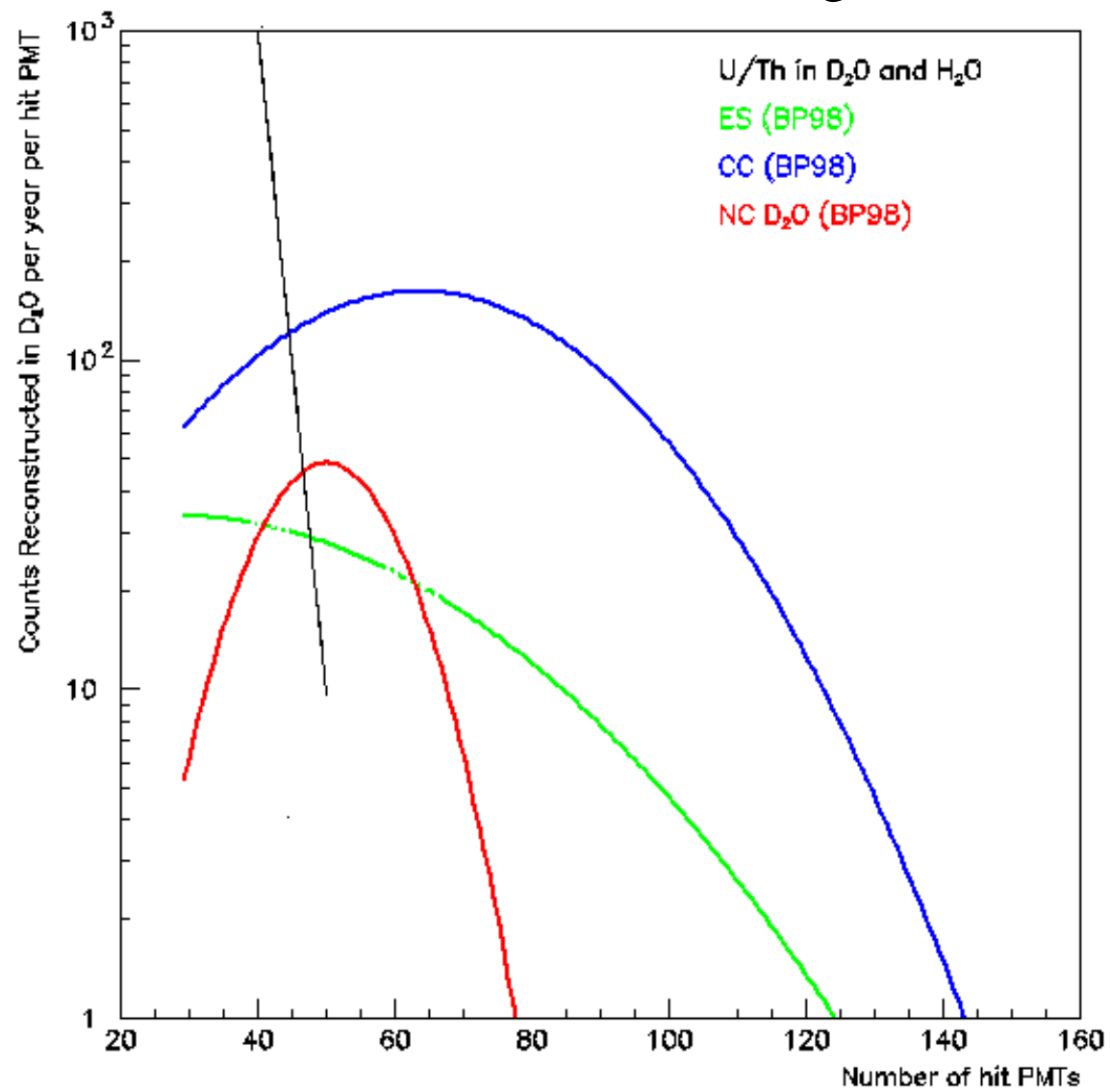
II. D20 + SALT

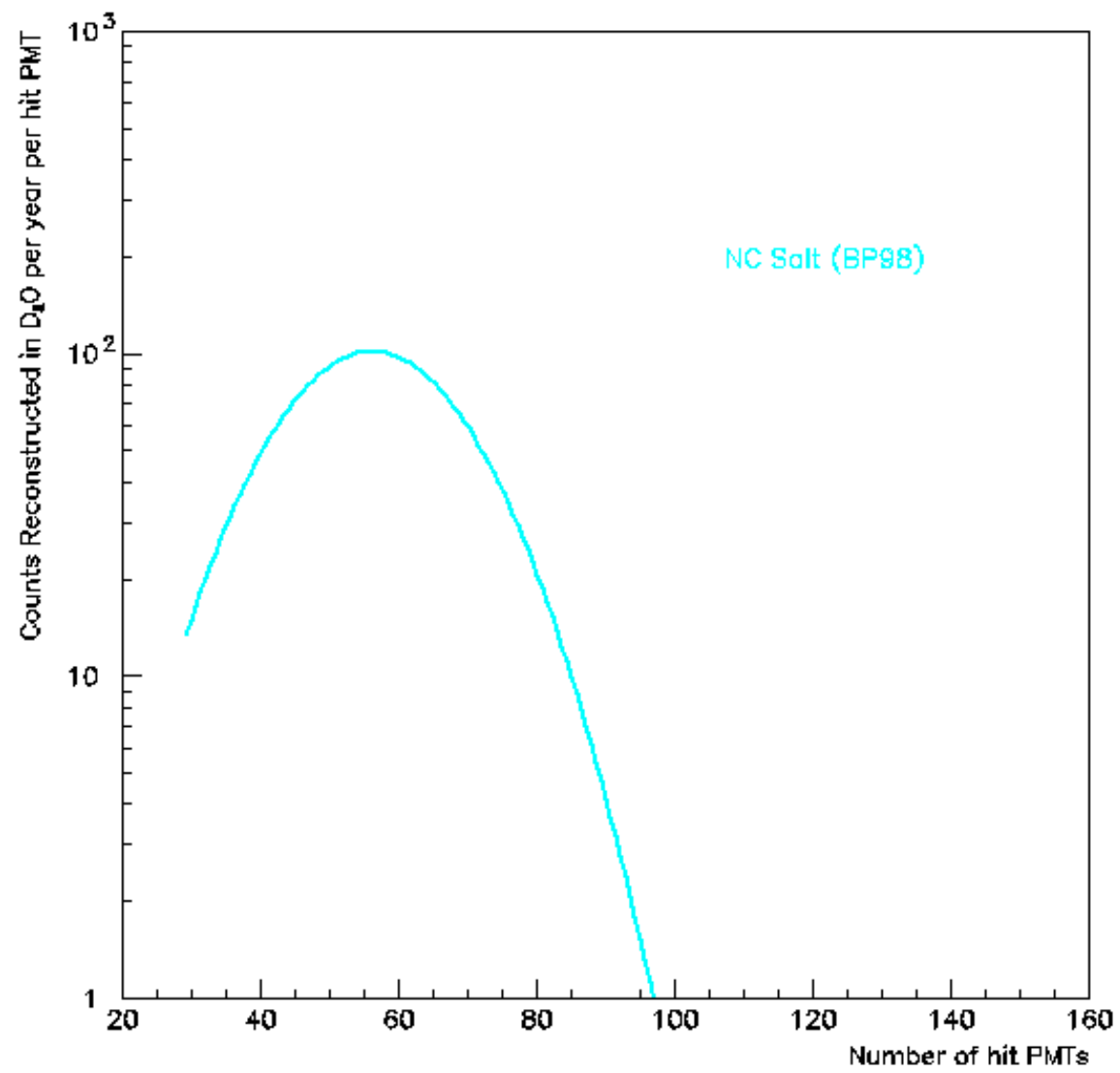
- ☀ Enhanced NC Sensitivity

III. D20 + NCDs

- ☀ Enhanced NC Sensitivity & Event-by-Event Separation of CC & NC

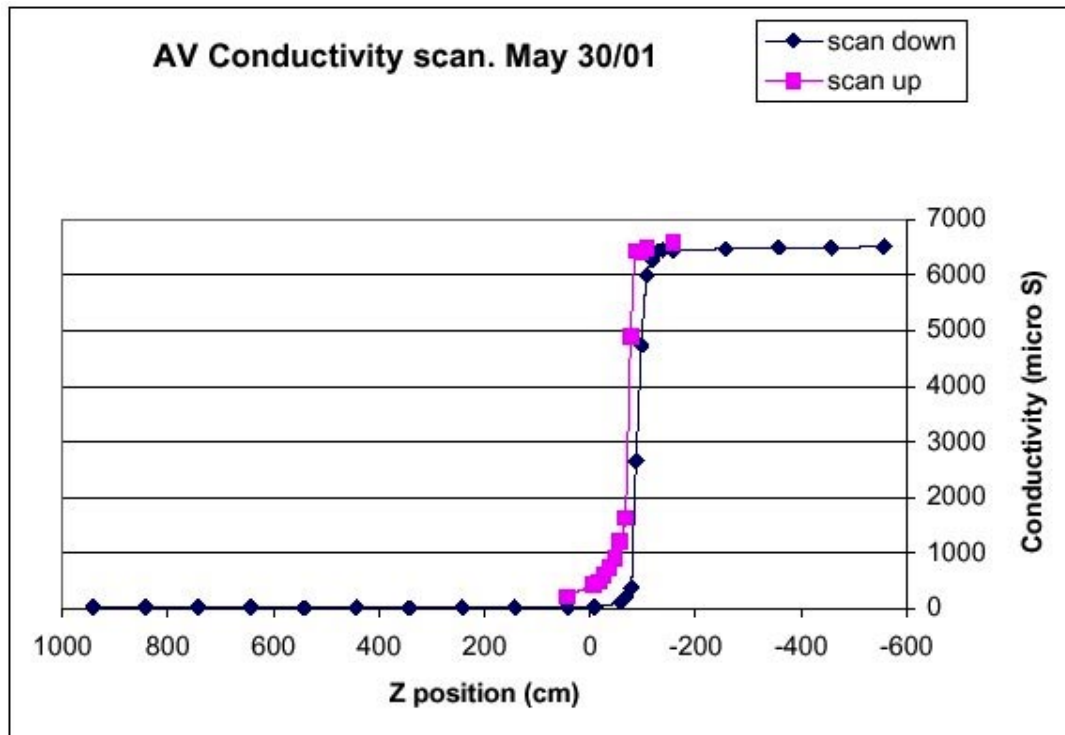
Monte Carlo of SNO Signals





Phase II Underway!!

NaCl Injected into D₂O. Calibrations in Progress.



Conductivity Measurements
Taken During Salt Addition

